Deciphering the potential niche of two novel black yeast fungi from a biological soil crust based on their genomes, phenotypes, and melanin regulation

Erin C. Carr[1], Quin Barton[2], Sarah Grambo[3], Mitchell Sullivan[1], Cecile M. Renfro[4], Alan Kuo[5], Jasmyn Pangilinan[5], Anna Lipzen[5], Keykhosrow Keymanesh[5], Emily Savage[5], Kerrie Barry[5], Igor V. Grigoriev[5,6], Wayne R. Riekhof[1], Steven D. Harris[7,8]

1) University of Nebraska-Lincoln, School of Biological Sciences, Lincoln, Nebraska 68588; 2) University of Nebraska-Lincoln, Department of Biochemistry, Lincoln, Nebraska 68588; 3) Iowa State University, Roy J. Carver Department of Biochemistry, Biophysics, and Molecular Biology, Ames, Iowa 50011; 4) University of Nebraska-Lincoln, Department of Agronomy and Horticulture, Lincoln, Nebraska 68588; 5) US Department of Energy Joint Genome Institute, Lawrence Berkley National Laboratory, Berkley, California 94720; 6) Department of Plant and Microbial Biology, University of California Berkeley, Berkeley, California 94720; 7) Iowa State University, Department of Plant Pathology and Microbiology, Ames, Iowa 50011; 8) Iowa State University, Department of Entomology Ames, Iowa 50011

Abstract

Black yeasts are polyextremotolerant fungi that contain high amounts of melanin in their cell wall and maintain a primarily yeast form. These fungi grow in xeric, nutrient deplete environments which implies that they require highly flexible metabolisms and the ability to form lichen-like mutualisms with nearby algae and bacteria. However, the exact ecological niche and interactions between these fungi and their surrounding community is not well understood. We have isolated two novel black yeast fungi of the genus *Exophiala*: *E. viscosium* and *E. limosus*, which are from dryland biological soil crusts. A combination of whole genome sequencing and various phenotyping experiments have been performed on these isolates to determine their fundamental niches within the biological soil crust consortium. Our results reveal that these *Exophiala* spp. are capable of utilizing a wide variety of carbon and nitrogen sources potentially from symbiotic microbes, they can withstand many abiotic stresses, and can potentially provide UV resistance to the crust community in the form of secreted melanin. Besides the identification of two novel species within the genus *Exophiala*, our study also provides new insight into the production and regulation of melanin in extremotolerant fungi.

Background

Polyextremotolerant fungi are a polyphyletic group that can be divided morphologically into black yeast and microcolonial/meristematic fungi types (Gostinčar et al., 2012). These two sub-types are distinct in their morphology; black yeast fungi are usually only yeasts but can be dimorphic, whereas microcolonial fungi are typically filamentous, pseudohyphal, or possess other unique morphologies such as spherical cells (Ametrano et al., 2017; De Hoog et al., 2003; Gostinčar et al., 2011). However, all polyextremotolerant fungi share the capacity to produce melanin, which presumably accounts for much of their polyextremotolerance. Most polyextremotolerant fungi are in the subdivision Pezizomycotina, residing mainly within Eurotiomycetes and Dothidiomycetes, but one could argue that any fully melanized fungus could be a polyextremotolerant fungi (Gostinčar et al., 2009).

Melanin is arguably a defining feature of polyextremotolerant fungi given that they form unmistakably black colonies. Because of its structure and association with the cell wall, melanin imbues polyextremotolerant fungi with resistance to multiple forms of stress. Most commonly known is

ultraviolet (UV) light resistance, as melanin absorbs light in the UV part of the spectrum (Kobayashi et al., 1993). However, melanin is also capable of absorbing reactive oxygen species (ROS), reactive nitrogen species (RNS), providing tolerance to toxic metals, reducing desiccation, and potentially using ionizing radiation as an energy source (Cordero & Casadevall, 2017; Dadachova et al., 2007; Gessler et al., 2014; Płonka & Grabacka, 2006; Zanne et al., 2020). Collectively, these functions of melanin are thought to enhance the ability of polyextremotolerant fungi to colonize habitats that are otherwise inhospitable to most forms of life.

The production of melanin is a key functional trait observed in fungi spanning the fungal kingdom (Bell & Wheeler, 1986; Zanne et al., 2020). The diverse protective functions of melanin (e.g., metal resistance, ROS and RNS tolerance, UV resistance) underscores its broad utility in mitigating the impacts of stress despite the potential cost of its synthesis (Schroeder et al., 2020). Fungi are capable of producing three different types of melanin: pheomelanin, allomelanin, and pyomelanin, all of which have their own independent biosynthetic pathways (Pal et al., 2014; Perez-Cuesta et al., 2020). Allomelanin, is formed from the polymerization of 1,8-DHN, which requires the use of polyketide synthase for initial steps in production (Perez-Cuesta et al., 2020; Płonka & Grabacka, 2006) (**Figure 1**). Pyomelanin and pheomelanin share an initial substrate of Tyrosine, but pheomelanin derives from L-DOPA, whereas pyomelanin is created via tyrosine degradation (Perez-Cuesta et al., 2020; Płonka & Grabacka, 2006) (**Figure 1**). Allomelanin and pheomelanin are often referred to as DHN melanin and DOPA melanin respectively, given their chemical precursors. Unfortunately, due to the unique characteristics of melanins and their association with larger biomolecules, we do not know the complete structure of any type of melanin (Cao et al., 2021). However, given that we do know their chemical constituents, it is possible to draw some inferences about the relationship between structure and function of a particular type of melanin. For instance, out of the three types of melanin fungi can produce, only pheomelanin has a chemical precursor, 5-CysDOPA, with both Nitrogen and Sulfur in its structure (Płonka & Grabacka, 2006). Notably, all three fungal melanins are synthesized via independent pathways, which enables the targeted use of chemical inhibitors to block one pathway without interfering with the others. For example, previous studies have extensively used the chemical melanin blockers kojic acid and phthalide to block pheomelanin and allomelanin respectively (Pal et al., 2014) (**Figure 1**). Use of these chemical blockers allowed previous studies to identify the primary melanin biosynthetic pathway employed by individual fungal species (Pal et al., 2014).

Polyextremotolerant fungi tend to occupy extreme niches such as rock surfaces, external brick and marble walls, soil surfaces, and even the inside of dishwashers (Gostinčar et al., 2009; Zupančič et al., 2016). Characteristic features of these environments includes the relative paucity of nutrients and the frequent presence of a community biofilm consisting of photosynthetic organisms and/or bacteria (Gostinčar et al., 2012). Strikingly, these species are rarely found alone in their habitats, which suggests that multi-species interactions between fungi, bacteria, and photosynthetic organisms underlie the formation and function of these communities. That is, the ability of polyextremotolerant fungi to successfully adapt to their niche must depend on complex yet poorly understood interactions with other microbes.

We have isolated two polyextremotolerant fungi from a biological soil crust (BSC) in B.C., Canada. These novel fungi are of the genus *Exophiala*, which has previously been found in BSCs (Bates et al., 2006). Biological soil crusts are unique dryland biofilms that form on the surface of xeric desert soils where little to no plants are able to grow (Belnap, 2003; Belnap et al., 2001). They are notable for their

extensive cyanobacteria population, which seeds the initial formation of all biological soil crusts and creates the main source of nitrogen for the rest of the community (Belnap, 2002). Once the initial crust is established, it is then inundated with a consortium of bacteria, fungi, algae, archaea, lichens, and mosses (Bates et al., 2010; Lan et al., 2012; Maier et al., 2016). This community is a permanent fixture on the land they occupy unless physically disturbed, much like other biofilms (Belnap & Eldridge, 2001; Donlan & Costerton, 2002). As a result of the desert conditions BSCs reside in, the microbes found there are constantly exposed to extreme abiotic factors which they must tolerate simultaneously (Bowker et al., 2010). Some of these abiotic extremes are: UV radiation (especially at higher altitudes and closer to the poles) (Bowker et al., 2002), desiccation and osmotic pressures (Rajeev et al., 2013), and temperature fluctuations both daily and annually (Belnap et al., 2001; Bowker et al., 2002; Pócs, 2009). Microbes that reside in these biological soil crusts have therefore adapted mechanisms to withstand these abiotic extremes.

An extensive amount of research has been dedicated to certain members of the biological soil crust community, but one such less studied microbe has been the "free-living" fungal taxa. These fungi are non-lichenized (Teixeira et al., 2017) yet are still thriving in an environment where there are no plants to infect or decompose (Belnap & Lange, 2003), and no obvious source of nutrients besides contributions from the other members of the biological soil crust community (Belnap & Lange, 2003). This would imply that even though these fungi are not lichenized per say, they would have to be engaging in lichen-like interactions with the biological soil crust community to obtain vital nutrients for proliferation. While the idea of transient interactions between non-lichenized fungi and other microbes has been floated by previous researchers in other systems (Gostinčar et al., 2012; Grube et al., 2015; Hom & Murray, 2014), it will be a difficult task to strongly confirm in biological soil crusts given their taxonomic complexity.

Despite the importance of microbial interactions in enabling the successful formation of BSCs in a niche characterized by poor nutrient and water availability, the fungal components of BSCs and their relative functions within the interaction network remain poorly understood. Here, we combine genome sequencing with computational tools and culture-based phenotyping to describe two new species of black yeast fungi associated with BSCs. We report on their carbon and nitrogen utilization profiles, stress responses, and lipid accumulation patterns. In addition, we characterize their capacity for melanin production and generate valuable insight into mechanisms that might be involved in regulating the synthesis of these compounds and how their melanin production contributes to the BSC community.

Methods

Fungal Strains and Media

Two novel species of fungi are described here: *Exophiala viscosium* CBS 148801 and *Exophiala limosus* CBS 148802. Their genomes and transcriptomes are deposited at the Department of Energy's (DOE) Joint Genome Institute (JGI) on their Mycocosm website under their genus species names, and the National Center for Biotechnological Information (NCBI) under accession numbers PRJNA501636 for *E. viscosium* and PRJNA501637 for *E. limosus.* Their type strains have been deposited to the Westerdijk institute for access to the scientific community. *E. viscosium* and *E. limosus* are typically grown in malt extract medium (MEA; see **Table 1** for media recipe) at room temperature in an Erlenmeyer flask at 1/10th the volume of the flask, shaking at 200 rpm. Additional strains used in this study were *Saccharomyces cerevisiae* ML440 and BY4741, and *E. dermatitidis* wild type (WT) strain ATCC 34100. *S.*

cerevisiae strains are grown in Yeast Peptone Dextrose medium (YPD; see **Table 1** for media recipe), and *E. dermatitidis* is grown in MEA.

Fungal isolation and identification methods

Fungi were isolated from public land in B.C., Canada. Soil samples were taken from the top 2 cm of biological soil crusts. A 0.1 g portion of the crust was re-suspended in 1 mL of water, ground with a sterile micropestle, and diluted with a dilution factor (DF) of 10 till they reached 10,000x dilution. Each dilution was then spread out onto two different MEA petri plate containing either no antibiotics or containing: Ampicillin (100 mg/L), Chloramphenicol (50 mg/L), Gentamycin (10 mg/L), and Cycloheximide (100 mg/L). The plates were then incubated in a Percival light incubator at 23 °C with a 12 hr light/dark cycle and examined daily using a dissection microscope to check for small black colonies. Once a potential black colony was seen, half of it was removed and transferred to a new MEA (no antibiotics) petri plate. It was vital to examine the plates daily, because even in the presence of antibiotics many unwanted fast-growing microbes would grow on the plates and cover up the slower growing polyextremotolerant fungal colonies. Once a pure culture of each isolate was grown up (approximately 2 weeks), they were preserved in 30% Glycerol and stored in the -80 °C freezer. DNA sequencing of amplified internal transcribed spacer (ITS) sequences was used to identify the isolates. DNA was extracted using the Qiagen DNeasy Powersoil DNA extraction kit. Primers used to isolate the ITS region were: ITS1- (5'-TCC GTA GGT GAA CCT GCG G-3') and ITS4- (5'-TCC TCC GCT TAT TGA TAT GC-3') (White et al., 1990). A BioRad MJ Mini Personal Thermal Cycler was used, with the program set as: 1) 95 °C for 5:00 (5 minutes), 2) 94 °C for 0:30 (30 seconds), 3) 55 °C for 0:30, 4) 72 °C for 1:30, 5) Return to 2 35 times, 6) 72 °C for 5:00. Resulting PCRs were then checked via gel electrophoresis in 1% agar run at 80 V for 1 hr. Isolated ITS regions were sequenced using the Eurofins sequencing facility, and the sequences were subsequently identified using the basic locally aligned search tool (BLAST) of the National Center for Biotechnological Information (NCBI) database to look for potential taxa matches.

DNA extraction and RNA extraction for whole genome sequencing

A Cetyltrimethylammonium bromide (CTAB) based DNA extraction method was performed to obtain high molecular weight DNA for whole genome sequencing. The DNA extraction method used was derived from (Cubero et al., 1999). Changes to the original protocol include switching PVPP for the same concentration of PVP, use of bead beating tubes with liquid nitrogen-frozen cells and the extraction buffer instead of a mortar and pestle for breaking open the cells, and heating up the elution buffer to 65 °C before eluting the final DNA. These changes were made to optimize the protocol for liquid-grown yeast cells instead of lichen material. Cells for the DNA extraction were grown up in 25 mL of liquid MEA in 250 mL Erlenmeyer flasks for 5 days, 1 mL of those grown cells was used for the DNA extraction after washing with water twice.

RNA was obtained using the Qiagen RNeasy mini kit (Cat. No. 74104). Cells were grown in 25 mL of three different liquid media types (MEA, YPD, and MNV; see **Table 1**) in 250 mL Erlenmeyer flasks at room temperature for 5 days, and 1-2 mL of cells were used for the RNA extraction. Cells were washed with DEPC-treated water and flash frozen in liquid nitrogen in 1.5 mL microcentrifuge tubes. RNA extraction was then performed according to the methods by the RNeasy kit.

Genome assembly and annotation

Both genomes and transcriptomes were sequenced using Illumina technology. For transcriptomes, a plate-based RNA sample prep was performed on the PerkinElmer Sciclone next generation sequencing (NGS) robotic liquid handling system using Illuminas TruSeq Stranded mRNA high throughput (HT) sample prep kit utilizing poly-A selection of mRNA following the protocol outlined by Illumina in their user guide: https://support.illumina.com/sequencing/sequencing_kits/truseq-stranded-mrna.html, and with the following conditions: total RNA starting material was 1 µg per sample and 8 cycles of PCR was used for library amplification. The prepared libraries were quantified using KAPA Biosystems' next-generation sequencing library qPCR kit and run on a Roche LightCycler 480 real-time PCR instrument. The libraries were then multiplexed and prepared for sequencing on the Illumina NovaSeq sequencer using NovaSeq XP v1 reagent kits, S4 flow cell, following a 2x150 indexed run recipe.

Using BBDuk (https://sourceforge.net/projects/bbmap/), raw reads were evaluated for artifact sequence by kmer matching (kmer=25), allowing 1 mismatch and detected artifact was trimmed from the 3' end of the reads. RNA spike-in reads, PhiX reads and reads containing any Ns were removed. Quality trimming was performed using the phred trimming method set at Q6. Finally, following trimming, reads under the length threshold were removed (minimum length 25 bases or 1/3 of the original read length - whichever is longer). Filtered reads were assembled into consensus sequences using Trinity ver. 2.3.2 (Grabherr et al., 2011).

For genomes, DNA library preparation for Illumina sequencing was performed on the PerkinElmer Sciclone NGS robotic liquid handling system using Kapa Biosystems library preparation kit. 200 ng of sample DNA was sheared to 300 bp using a Covaris LE220 focused-ultrasonicator. The sheared DNA fragments were size selected by double-SPRI and then the selected fragments were end-repaired, A-tailed, and ligated with Illumina compatible sequencing adaptors from IDT containing a unique molecular index barcode for each sample library. The prepared libraries were quantified using KAPA Biosystems' next-generation sequencing library qPCR kit and run on a Roche LightCycler 480 real-time PCR instrument. The quantified libraries were then multiplexed with other libraries, and the pool of libraries was then prepared for sequencing on the Illumina HiSeq sequencing platform utilizing a TruSeq paired-end cluster kit, v4, and Illumina's cBot instrument to generate a clustered flow cell for sequencing. Sequencing of the flow cell was performed on the Illumina HiSeq2500 sequencer using HiSeq TruSeq SBS sequencing kits, v4, following a 2x150 indexed run recipe.

An initial assembly of the target genome was generated using VelvetOptimiser version 2.1.7 (3) with Velvet version 1.2.07 (Zerbino & Birney, 2008) using the following parameters; "--s 61 --e 97 --i 4 --t 4, --o "-ins_length 250 -min_contig_lgth 500"". The resulting assembly was used to simulate 28X of a 2x100 bp 3000 +/- 300bp insert long mate-pair library with wgsim version 0.3.1-r13 (https://github.com/lh3/wgsim) using "-e 0 -1 100 -2 100 -r 0 -R 0 -X 0 -d 3000 -s 30". 25X of the simulated long mate-pair was then co-assembled together with 125X of the original Illumina filtered fastq with AllPathsLG release version R49403 (Gnerre et al., 2011) to produce the final nuclear assembly. The genome was annotated using JGI Annotation pipeline (Grigoriev et al., 2014). The assemblies and annotations of both genomes are available at the fungal genome portal MycoCosm ((Grigoriev et al., 2014); https://mycocosm.jgi.doe.gov) and in the DDBJ/EMBL/GenBank repository under accessions X and X.

Phylogenetic analysis

Our approximate maximum likelihood phylogenetic tree was constructed from the protein sequences of 24 taxa which represent a sampling of the family Herpotrichielleaceae in which *E. viscosium* and *E. limosus* reside. We created this tree using the pipeline described in Kuo et al. (Kuo et al., 2014). We wanted to obtain the largest set of data for phylogenetic analysis available by defining homologous proteins across all 24 genomes using Best Bidirectional Blast pairs via BlastP across all proteins of all the genomes from their FilteredModels or ExternalModels files available on Mycocsm. Resulting defined homologous proteins across all 24 genomes were then used as our sequences for the rest of the pipeline. These sequences were aligned with Mafft v7.123b with no alterations (Katoh et al., 2002). That alignment was then trimmed using Gblocks 0.91b with options -b4=5 -b5=h to have a minimum of 5 positions per block and allowing up to half of those to be gaps (Castresana, 2000). The resulting trimmed alignment was then input into FastTree version 2.1.5 SSE3 with options -gamma -wag (Price et al., 2009). The tree file was then input into iTOL for visual optimization (Letunic & Bork, 2021).

Mating type locus identification

Mating loci for *E. viscosium* and *E. limosus* were determined using the methods described by (Teixeira et al., 2017). Genes known to flank the MAT loci of most Chaetothyriales species include: *APN2*, *SLA2*, *APC5*, and *COX13*. The protein sequences of these genes from *Aspergillus nidulans* were used to BLASTP against the genomes of the new fungi. These gene sequences were obtained from Aspergillus Genome Database and BLASTed using JGI's Mycocosm. Once those genes were found, analysis of upstream and downstream flanking genes was performed until the mating gene MAT1-1 was located. Genes close to MAT1-1 and within the span of genes listed above were considered part of the MAT locus.

Phenotyping experiments:

Characterization of *E. viscosium* and *E. limosus* was performed to provide us with the knowledge of these new species' capabilities. Experiments performed were carbon utilization, nitrogen utilization, UV resistance, metal resistance, growth temperature range, budding patterns, lipid profiles, and growth capabilities on various fungal medias as described below.

Budding Pattern determination

Protocols for observing the budding patterns of these new species were derived from methods in (Mitchison-Field et al., 2019). A 1:1:1 ratio by weight of Vaseline, Parafin, and Lanolin (VALAP) was combined in a glass bottle and heated to 115 °C to melt completely and kept at room temperature for later use. Heated solid MEA was aliquoted into a 50mL tube for agar slab making. Isolates were grown in liquid MEA for 5 days prior to inoculation of slides. First, the VALAP was brought back up to 115 °C to melt completely for application. Then 5 µL of the 5-day old cells were diluted in 995 µL of liquid MEA. Agar slabs of MEA were made by microwaving the 50 mL tube of solid MEA until it melted, then pipetting 1 mL of the hot agar into a 1 cm x 2 cm mold formed out of cut strips of silicone and laid down in a sterile petri dish. This agar slab was allowed to solidify and was then cut in half to be 1 cm x 1 cm. Both the cover slip and the slide were wiped down with ethanol to ensure clean and sterile growth conditions for the cells. 8 µL of the diluted cells was pipetted onto the center of the sterile slide, then one square of the agar slab was carefully placed on top of the cells in media, 8 µL of MEA was pipetted onto the top of the agar slab, and the coverslip was placed over the agar slab. Using a small paintbrush, the melted VALAP was carefully painted onto the gap between the coverslip and the microscope slide to

seal off the coverslip. Finally, a 23-gauge needle was used to poke holes in the solidified VALAP to allow for gas exchange.

The slide was then placed with the slide facing down onto the inverted microscope EVOS fl. Once an adequate number of cells was observed in frame, the cells were allowed to settle for 2 hours before imaging began. Images were then automatically taken every 30 mins for 72 hours. Videos of the budding pattern were created using Adobe Premiere Pro.

Growth of E. viscosium and E. limosus on different medias

Eight different fungal media were used to observe the growth of these novel fungi. These media have been used for identification purposes and will be useful for future identification of these species from other locations. Media used in this experiment were: MAG, MEA, MN, MNV, MN+NAG, PDA, Spider, YPD, V8 (**Table 1**). Both isolates were first grown in 25 mL of liquid MEA at room temperature, shaking at 200 rpm for 5 days. Then 1 mL of each species was aliquoted and washed 3 times with water. Washed cells were then applied to the media in three ways: 5 µL spotting (pipetting 5 µL of cells onto the plate), toothpick poking (poking a sterile toothpick tip into the suspended cells and then onto a plate), and metal loop streaking (placing sterile metal loop into suspended cells, then spreading cells onto plate in a decreasing manner). This provided us with different plating techniques that could potentially yield different morphologies.

Carbon Utilization

Carbon utilization of each isolate was determined using a BioMerieux ID C32 carbon utilization strip (Cat. No. 32200-1004439110). These strips have 30 different carbon sources in individual wells, one well with no carbon source for a negative control, and one well with Ferric citrate. The inoculated strips were kept in a plastic box container with a lid and lined with moist paper towels to reduce drying. The initial inoculum of cells was prepared in 25 mL of MEA shaking at room temp for 5 days. Inoculation of the strips was done according to the instructions provided by the vendor, and each strain was inoculated in three separate strips for triplicate replication. Cells were diluted to the kit requirement of McFarland standard #3 (McFarland, 1907) before starting the inoculum. Growth in the ID strip lasted 10 days before evaluation. Growth in each well was observed and evaluated by eye. Each well was compared to the negative control (no carbon) and the positive control (dextrose). Initial growth was evaluated on a: +, V, -, and - - scale. If a well had the same growth as the negative control it was given a "-", meaning no growth; if the well had less growth than the negative control it was given a "- -", meaning growth was inhibited by the carbon source; if a well had growth equal to or more than the dextrose well then it was given "+", meaning it was capable of growth on the carbon substrate; finally if the well was in between the negative control and positive control it was given a "V", for variable growth. Nuances of the fungal growth on individual carbon sources required a more gradual scale, and so scores were adjusted to form a range of 1-5 to allow for more accurate average calculation between the three replicates. For this scale: one was no growth or equal to the kits "-", five was the most growth and equivalent to the kit's "+"; numbers in between allowed us to average out the replicates to ensure we had a sliding scale of utilization rather than multiple variable "V" utilizations without a clear idea of how variable the utilization was.

Nitrogen utilization

Nitrogen utilization tests were performed using ten different nitrogen conditions. 100 mM was the concentration used for all compounds that contained one nitrogen atom per molecule: Proline, Ammonium tartrate dibasic, Serine, Sodium Nitrate, Glycine, Glutamate, and Aspartate; 50 mM was the concentration used for Urea because it has two atoms of nitrogen per molecule; 1% w/v of Peptone was used as a positive control; and no nitrogen was added as a condition for a negative control (**Table 2**). Liquid minimal media (MN) with MN salts (not 20x Nitrate salts) was used with the varying nitrogen sources to ensure that no alternative nitrogen source would be available to the fungi. Fungi were first grown up in liquid MEA for 5 days at room temperature to reach maximum density. Then, 1 mL of cells was removed and washed three times with water. 99 µL of each nitrogen source-containing medium was added to six wells in a 96-well plate, for six replicates, and 1 µL of the washed cells was added to each well. 100 µL of each medium was also added to one well each without cells to blank each condition, because the different nitrogen sources created different colors of medium. Daily growth was measured from day 0 to day 7 at 420 nm, using the BioTek Synergy H1 hybrid spectrophotometer.

Optimal growth temperature and range of growth temperatures

To determine the temperature resistance range and optimal growth temperature for each isolate, we grew both fungi at 4 °C, 15 °C, 23 °C (i.e., ambient room temperature), 28 °C, 37 °C, and 42 °C. Isolates were first grown up in 25 mL of MEA for 5 days at room temperature to maximum density. Then 1 mL of cells was removed, and a 10x serial dilution was made from 0x to 100,000x, using pre-filled 1.5mL tubes with 900 µL of MEA and adding 100 µL of the previous tubes each time. Then 5 µL of each serial dilution was spotted onto a square MEA plate which allowed us to determine the carrying capacity of each isolate at the different temperatures. Plates were kept at their respective temperatures for 7 days before observations were made, however the 37 °C and 42 °C incubators required cups of water inside of them to prevent the plates from dehydrating. Plates grown in 42 °C and 37 °C were then allowed to grow at room temp for up to a week to determine if the isolates died at these temperatures or if their growth was just arrested.

UV resistance

Resistance to UV light was observed to determine if these black fungi, with highly melanized cell walls and constant exposure to sunlight in their natural habitat, were in fact UV resistant. To determine this, we used the UVP HL-2000 HybriLinker UV crosslinker as our source of UV light, which has a UV wavelength of 254 nm. Lower wavelengths (100-280 nm) are of the UV-C range, they are considered ionizing radiation and are the most detrimental to living organisms, but are completely blocked by the ozone layer (Molina & Molina, 1986; Schreier et al., 2015). Therefore, using this wavelength we are able to push our organisms beyond the UV limits found in their natural habitat and test extreme amounts of UV exposure. The fungi were inoculated in 25 mL of MEA in a 250 mL Erlenmeyer flask and let grow under shaking conditions at 200 rpm for 5 days at room temperature to reach maximum density. 100 µL of this culture was then spread out onto 6 MEA plates, using a glass spreader. Three plates were kept as the control growth, to compare to the three other plates which were exposed to the UV light. Experimental plates were placed inside of the crosslinker with their lids taken off. Then the plates were exposed to 120 seconds of UV light from a distance of 9.5 cm to the light source at 10,000 µJ/cm^2 (254 nm) (Frases et al., 2007). We then wrapped all plates in aluminum foil and placed them in the Percival light incubator set at 23 °C for 2 days. Placing UV-exposed cells in complete dark after exposure is essential for preventing native cell repair mechanisms to act upon any potential mutations, allowing for

only those cells that are capable of withstanding the UV exposure without repair mechanisms to grow (Weber, 2005). After 2 days the plates were removed from the aluminum foil and left in the incubator for 5 more days before final observations. To determine whether a particular isolate was resistant to UV exposure, the growth of the isolate exposed to UV was compared to the control growth.

Metal Resistance

Metal resistance is a relatively universal trait in many polyextremotolerant fungal species. Due to the under-studied nature of this particular characteristic in biological soil crusts and fungi, we decided to test if any of our isolates were resistant to any heavy metals which would indicate possible bioremediation capacity. In order to test metal resistance, we used the antibiotic disc method by aliquoting metal solutions onto paper discs and observing zones of clearance. Metals and concentrations used are listed in **Table 3.** For testing, 5 µL of each metal solution was aliquoted onto a dry autoclaved Wattman filter paper disc which was created using a standard hole puncher. These discs were then allowed to air dry and kept at 4 °C for up to a week. Initial growth of the fungal isolates was done in 25 mL of MEA, shaking at 200 rpm for 5 days at room temperature. We then spread 100 µL of each fungal isolate onto 100 mm sized MEA plates using a glass spreader to create a lawn. Using flame sterilized tongs our metal paper discs were placed onto the center of the petri dish on top of the fungal lawn and lightly pressed down to ensure the metal disc was touching the plate completely. These plates were then placed in the Percival light incubator at 23 °C with a 12 hr light/dark cycle for up to 2 weeks. Once a zone of clearing was clearly visible amongst the fungal growth (1-2 weeks), the zone of clearing was then measured in cm. Generally, large zones of clearing indicated sensitivity to the metal, whereas zones of reduced size were consisted with resistance to the metal.

Lipid profiles

Comparison of the lipid production of *S. cerevisiae*, *E. dermatitidis*, *E. viscosium*, and *E. limosus* was performed in the presence of fermentable vs. non-fermentable sugars in high and low nitrogen. To test these conditions we grew all four species in four different media types. 1) MEA; 2) MEA + 20 g/L of peptone instead of 2 g/L; 3) MEA with the dextrose replaced with the same weight amount of glycerol; 4) MEA with glycerol instead of dextrose and 20 g/L of peptone instead of 2 g/L. All four fungal species were first inoculated in 25 mL of liquid MEA in a 250 mL Erlenmeyer flask and shaken at 200 rpm for 5 days at room temperature to reach peak density. Then 100 µL was inoculated into 5 mL of each media in a size 25 mm tube, placed in a roller drum and allowed to grow at room temperature for 5 days.

To observe their lipid profile, we performed a standard Bligh Dyer lipid extraction (Bligh & Dyer, 1959). Equal wet weight of each organisms' cells was pelleted and re-suspended in 2 mL of methanol inside of 16 mm glass tubes. Tube openings were covered in Durafilm before applying the lid of the tube, then samples were boiled for 5 minutes and let cool for 10 minutes. Then 2 mL of chloroform and 1.6 mL of 0.9% NaCl were added, and the tubes were vortexed to fully mix. Tubes were then centrifuged at 5000 rpm for 5 minutes to separate the layers. The bottom lipid layer of the suspension was removed and placed in a new glass tube which was then dehydrated using nitrogen gas till the samples became fully dry. Dehydrated samples were then re-suspended with 100 µL of a 9:1 ratio of chloroform : methanol to run the thin layer chromatography (TLC) with. For all samples except the *S. cerevisiae*, 7 µL of the lipid suspension was used to dot the TLC. For *S. cerevisiae,* 10 µL of the lipid suspension was needed. The solvent systems used for TLC were Chloroform : methanol : glacial acetic acid: water 85:12.5:12.5:3 for the Polar lipid solvent system, and Petroleum ether : Diethyl ether : acetic acid 80:20:1 for the neutral

lipid solvent system. The TLC plates were loaded with 7 or 10 µL of the re-suspended samples, and they were placed in the Polar solvent system for approximately 30 minutes (half-way up the plate) before transferring to the Neutral Lipid solvent system in a separate container till the solvent front reached just a few cm below the top of the plate. The plate was then removed and dried for 15 minutes, until the solution on the plate was no longer volatile, and the plate was placed in the presence of iodine (Sigma-Aldrich cat. No. 207772) in a glass chamber for 5 minutes until all the lipids were visible. The plates were then immediately placed in plastic covers and scanned and photographed for visualization and documentation.

Melanin experiments:

Melanin biosynthesis gene annotation

Melanin biosynthesis in fungi occurs via three different pathways: the DHN pathway which creates allomelanin, the DOPA pathway which creates pheomelanin, and the tyrosine degradation pathway which creates pyomelanin (Cao et al., 2021; Gessler et al., 2014). Most fungal species only contain one melanin biosynthetic pathway, but there are many species in Pezizomycotina, particularly in the genera *Aspergillus* and *Exophiala*, which are capable of producing two or all three forms of melanin (Teixeira et al., 2017). For that reason, we decided to manually annotate the genes involved in all three melanin biosynthetic pathways in *E. viscosium* and *E. limosus* to determine if they too possessed all three melanin biosynthetic pathways. In all cases, the relevant *A. niger* genes were used as queries (Teixeira et al., 2017). Protein sequences for each gene were found using the Aspergillus genome database (AspGD) and were tested using BLAST-P against the filtered model proteins database of *E. viscosium and E. limosus* on Mycocosm. Since *A. niger* contains paralogs for some melanin biosynthetic genes, all genes listed in (Teixeira et al., 2017) were used as queries for BLAST searches. Once the melanin biosynthetic genes in *E. viscosium* and *E. limosus* were identified, their highest matching protein sequences were then reverse BLASTed to the *A. niger* genome to determine the reciprocal best hit and ensure true homology.

Regulation of Melanin production using chemical blockers

Once it was established that both isolates contain the potential for production of all three fungal melanins, the effects of known chemical blockers of the DHN and DOPA melanin pathways was used to investigate melanin production. DHN melanin blocker Phthalide and the DOPA melanin blocker Kojic acid were both used in hopes of blocking melanin production in these isolates. Stock solutions were made according to (Pal et al., 2014): Phthalide was diluted in 70% ethanol, and Kojic acid in DMSO. Three separate experiments were performed using these melanin blockers, to determine which method would provide the most informative results.

The first was the disc diffusion method whereby Whatman filter paper discs were autoclaved and impregnated with 5 µL of either 10 mM of Phthalide or 10 mg/mL of Kojic acid. Impregnated filter paper discs were then placed on top of freshly spread lawns of either isolates on both MEA and YPD. Lawns were of 50:50 diluted 5-day old cells grown in MEA, and 100 µL of this dilution was spread onto the petri plates with a glass spreader. These plates were then grown at 23 °C with 12 hr light/dark cycles for 5 days. Additionally, both a Kojic acid disc and Phthalid discs were placed on fungal lawns ~4 cm apart simultaneously to observe their specific melanin-blocking capabilities on the same cells.

Next, we tried adding the melanin blockers directly to the medium as was done in (Pal et al., 2014). Since melanin is more universally distributed in *Exophiala* cells compared to *Aspergillus* cells, we decided to use the highest concentration of both Kojic acid and Phthalide that was used by (Pal et al., 2014), which was 100 mM of each compound. This concentration was added to both solid YPD and MEA after autoclaving, individually and combined. These plates were then used for two forms of growth experiments. Alternatively, we spread a lawn onto YPD and MEA with and without Kojic acid, Phthalide, and both compounds at 100 mM each. Finally, we performed a 10x serial dilution of both *E. viscosium* and *E. limosus* up to 10,000x diluted, and spotted 5 µL of each dilution onto MEA plates with and without Kojic acid, Phthalide, and both compounds. We let both growth experiments grow at 23 °C for 5 days with a 12 hr light/dark cycle.

Melanin Extraction and spectrophotometric measurements

Extraction of melanin from a variety of sources has been performed with two main categories of methods: chemical extraction and enzymatic extraction (Pralea et al., 2019). We were unsure which extraction method would be most applicable to these species, so both were performed. The enzymatic extraction method that was used came from (Rosas et al.) (2000). Alternatively, the chemical extraction method, which has been used more extensively in previous works, was derived from (Pal et al., 2014). Their method for extraction and purification of melanin from culture filtrate was adapted and used for all future secreted melanin extractions. Adjustments to the Pal et al. method included: the 6M HCl precipitation took multiple days instead of overnight for melanin to precipitate, then stopping the protocol when 2M NaOH was added to the extracted melanin. We did not continue on to re-precipitation and drying of the melanin as this product did not reprecipitate in any solvents used.

Exact methods are as follows. 10 mL of culture was centrifuged at 3,000x g for 5 minutes, and the resulting supernatant was filter sterilized through a 2 µm filter to ensure all cells were removed. The filtered supernatant was then transferred into a 50 mL centrifuge tube, and 40 mL of 6M HCl was added to the tube. The filtrate was then allowed to precipitate out for up to two weeks. Precipitated solutions were then centrifuged at 4000 rpm for 3 minutes, and the resulting supernatant was discarded. The pellet was washed with 2 mL of dd H_2O, vortexed, centrifuged, and the supernatant discarded. Then 3 mL of 1:1:1 Chloroform : ethyl acetate : ethanol was added to the samples and vortexed vigorously to ensure as much re-distribution of the melanin was accomplished. The tubes were then centrifuged again, and any resulting clear layers (top and or bottom) were discarded, leaving behind the dark layer. 2 mL of water was added to the sample for washing, and the tubes were centrifuged again, and the entire supernatant was discarded. Finally, 1 mL of 2M NaOH was added to each sample to allow for a standard volume added even if the melanin amount and therefore the final volume varied.

Extracted melanin samples suspended in 1 mL of 2M NaOH were then diluted 5 µL into 195 µL of 2M NaOH into a 96-well plate, with a 200 µL 2M NaOH blank well. These diluted samples were then read using the BioTek Synergy H1 hybrid spectrophotometer. The settings were for a full spectrum read from 230 nm to 700 nm, with 10 nm steps. However, the machine could not read ODs above 4.0, and therefore only data from 300 nm to 700 nm was used.

Melanin secretion and its concentration in the supernatant

To confirm that *E. viscosium* and *E. limosus* are actively secreting melanin, as opposed to dead cells lysing and releasing it, we grew up both species and took daily aliquots for melanin extraction.

Additionally, we wanted to compare the melanin secretion capabilities of these species to *E. dermatitidis* for a baseline comparison. All three species were grown up in liquid MEA shaking at room temperature for 5 days. Then 2 mL of cells were washed with water three times. 500 µL of washed cells were then inoculated into 100 mL of MEA and YPD in 500 mL flasks. We let the cells grow at 23 °C shaking at 200 rpm for 7 days, removing 11 mL of cells and supernatant daily and pipetting them into 15 mL centrifuge tubes. The tubes of cells were then centrifuged at 3000 rpm for 5 minutes, the supernatant was removed, filter sterilized through a 2 µm filter, and placed into a new tube. We filter sterilized the supernatant to ensure that no cells remained in the supernatant, therefore all of the melanin extracted came only from secreted melanin. Melanin was then extracted using the chemical method explained above. Resulting pure melanin for all samples was read with the full spectrum as stated above, and both standard OD and log scale graph were created to confirm the presence of melanin with the proper R^2 value above 0.9 (Pralea et al., 2019).

Increasing amounts of peptone

To assess the role of nitrogen levels in melanin secretion, we initially switched the concentration of peptone added to YPD and MEA media; the new media would be: YPD + 0.2% peptone, and MEA + 2% peptone. We then took both *E. viscosium* and *E. limosus* that was grown in liquid MEA for 5 days shaking at room temperature and plated out the species onto these new media using the same technique as described above for growth comparison on different media. To determine if a more gradual increase in peptone would correlate with a gradual secretion of melanin, we took the base media of MEA (solid) and changed the concentration of peptone to: 0.1%, 0.5%, 1%, 1.5%, 2%, 2.5%, 3%, 3.5%, 4%, and 5%. We then spotted 5 µL of both species onto the plates after performing a 10x serial dilution up to 10,000x dilution. The plates were grown at 23° for 10 days with a 12 hr light/dark cycle.

Albino mutant experiments:

Creation of EMS mutants and annotation of their mutations

Genetic modification of these species has not been established yet. However, random mutagenesis via chemical mutagens was performed in the hopes of finding albino mutants, to provide greater insight into the regulation of melanin production. UV exposure which is used frequently as a mutagen for random mutagenesis was attempted, but never resulted in phenotypically distinct mutants or albino mutants. Instead, we used ethyl methyl sulfonate (EMS) to induce G:C to A:T mutations randomly within the genomes of our two species. This was performed using the method by (Winston, 2008). Albino mutants and other interesting pigmentation or morphological mutants were isolated from the resulting mutagenesis, and their DNA was extracted using the same CTAB extraction manner stated above. Their DNA was then sent to the Microbial Genome Sequencing Center (MiGS) for genome re-sequencing and base-called against the wild-type DNA. Resulting mutations were then manually annotated using the JGI Mycocosm genome “search” tool to determine if any genes were disrupted by the mutations to cause the phenotype observed.

Recovery of melanin production in albino mutants

Following recovery of our albino mutant, we attempted to restore melanin production via chemical induction of the other melanin biosynthetic pathways. We did this using hydroxyurea (HU), L-DOPA, and 1,8-DHN. Hydroxyurea has been shown to enhance melanin production in *E. dermatitidis*, and L-DOPA is

needed for certain fungi to produce melanized structures, including the albino mutant form of *E. dermatitidis* WdPKS1 (Dadachova et al., 2007; Paolo et al., 2006; Schultzhaus et al., 2020). Both YPD and MEA medium was made up and 20 mM of HU, 1 mM of L-DOPA, or 1 mM of 1,8-DHN was added to the medium after autoclaving. Our albino mutant was then grown up in the same way as our wild type cells. 5 µL of grown cells were spotted onto these media with added compounds and they were grown for 10 days at 23 °C 12 hr light/dark cycle.

Results

Description of *Exophiala viscosium* and *Exophiala limosus*

Exophiala viscosium CBS 148801 was isolated from Jackman Flats Provincial Park in B.C. Canada. Initial ITS sequencing was performed to obtain potential taxonomic matches. BLAST results to its ITS sequence matched 97.57% to "*Exophiala nigra* strain CBS 535.95" accession number: MH862481.1. Whole genome sequencing and further phylogenetic analyses subsequently revealed that *E. viscosium* is a novel species closely related to *E. sideris* (**Figure 2**).

Morphological characterization of *E. viscosium* demonstrated that compared to *E. dermatitidis*, *E. viscosium* has much darker pigmentation, and is also a more viscous cell culture. When scraping a colony off the plate it comes up like stretchy tar usually leaving a string of cells hanging off the sterile loop. *E. viscosium* does not disperse in water easily when re-suspending, but it does pellet easily at 10,000x g for 1 minute. When grown up on a MEA plate for a week or more, it will begin to form a rainbow sheen like an oil slick (**Figure 3A**). Hyphal growth will begin to form into the agar when the plate is left alone at room temperature for more than three weeks. Interestingly, secretion of melanin into the agar can be observed after two weeks on MEA and one week on YPD plates. In liquid culture, this occurs more quickly, with melanin observed in the supernatant starting at 5 days in MEA and 3 days in YPD. The cellular morphology of *E. viscosium* is that of a true yeast. It has large tear-drop shaped cells that usually bud one at a time but can sometimes bud 2-3 times simultaneously (**Figure 3B**). Lipid bodies are frequently observed, as the large circles within cells (**Figure 3B**) and have been confirmed by Nile red staining (data not shown). This isolate grows to its maximum density in 7 days at 23 °C in 25 mL of MEA in a 250 mL Erlenmeyer flask shaken at 200 rpm. *Exophiala viscosium* was originally referred to as "Goopy" due to the nature of its morphology. Accordingly, we have formally named it *Exophiala viscosium* for the Latin term of viscous.

Exophiala limosus CBS 148802 was isolated from a biological soil crust on public land in B.C. Canada. The ITS region of *E. limosus* most strongly matched "*Exophiala nigra* strain CBS 535.95" accession number: MH862481.1 with an identify of 97.67%. Although both *E. viscosium* and *E. limosus* have similar phylogenetic placement, their cellular morphology and budding patterns differ drastically (**Figures 3** & **5**). As seen in **Figure 3D**, the cellular morphology of *E. limosus'* resembles that of *Horatea werneckii* as observed by (Mitchison-Field et al., 2019). Cells are more elongated than *E. viscosium*, and when grown up to maximum density pipetting becomes difficult due to large clumps of cells formed by its more filamentous growth pattern. Both isolates have the consistency of sticky black tar, and an iridescent shine that forms after a week on an MEA plate. *Exophiala limosus* also fails to easily disperse when suspended in water but can be readily pelleted. These observations and the prominence of lipid bodies within the cells (**Figure 3D**) suggests that lipid-derived compounds could cause their sticky, water repelling, iridescent nature. This isolate grows to its maximum density in 7 days at 23 °C in 25 mL of MEA

in a 250 mL Erlenmeyer flask shaken at 200 rpm. Originally, *E. limosus* was named "Slimy" to reflect its colony characteristics. Accordingly, we have formally named it *Exophiala limosus* for the Latin term of muddy. Notably, *E. limosus* possesses a looser pellet and is less refractory to re-suspension than *E. viscosium*.

Genome description

The genome assembly sizes of these two novel *Exophiala* species are: 28.29 Mbp for *E. viscosium* and 28.23 Mbp for *E. limosus* (**Table 4**). These sizes are similar to other yeasts in the genus *Exophiala* and are only a bit smaller than their closest relative *E. sideris* (29.51 Mbp). Although their genomes are smaller than *E. sideris*, predicted gene content is relatively higher; 11344 for *E. viscosium* and 11358 for *E. limosus* as compared to 11120 for *E. sideris* (**Table 4**). However, *E. sideris* appears to possess longer genes, transcripts, exons, and introns compared to *E. limosus* and *E. viscosium,* which could also contribute to the gene number to genome size differences (**Table 4**). *E. viscosium* contains the highest GC% amongst the *Exophiala* species listed in **Table 4**. *E. viscosium*'s GC content is even higher than *E. limosus* by 2.65%, which given their genetic similarities is quite interesting.

Mating type

Exophiala species are one of the many fungal genera whose mating capabilities remain incompletely understood and vary across the genus (Teixeira et al., 2017). The closest species to *E. viscosium* and *E. limosus* is *E. sideris,* within which both mating types have been characterized as a single fused gene (Teixeira et al., 2017). Given the known order of genes in regions flanking the MAT locus in *Exophiala* species, we used comparative approaches to determine the mating identities of the sequenced *E. viscosium* and *E. limosus* isolates, and to look for possible evidence of homothallism that is also presumed in *E. sideris*. Homologues of the genes *APN2*, *SLA2*, *APC5*, *COX13*, and *MAT1* (*MAT1-1/alpha*) in *E. viscosium* and *E. limosus* were identified via BLAST searches. We found that *APN2* and *SLA2* flank the *MAT* gene of both species, and they also contain the Herpotrichalleaceae-specific mating gene *MAT1-1-4* (**Figure 4**). These results are not surprising, in that this is the exact same order of these genes in *E. sideris*. Interestingly, as Teixeira et al. indicate, in *E. sideris* the *MAT* gene is a fused *MAT1-1/MAT1-2* gene with the HMG domain in the middle splitting the α-box in half (Teixeira et al., 2017). When the MAT gene protein sequences of *E. viscosium* and *E. limosus* are aligned with the *MAT* gene of *E. sideris*, we see very high homology indicating that these fungi also contain a fused *MAT* gene. This fused *MAT* gene is theorized to allow these species to be homothallic, although this has not been confirmed experimentally in any of these three species. Additionally, neither *E. viscosium* nor *E. limosus* contain an additional gene between *APN2* and the *MAT1-1-4* that is found in *E. sideris* (Teixeira et al., 2017). Furthermore, *COX13* and *APC5* are about 7,000 bp downstream of the MAT locus in both species, but *COX13* is on the opposite strand in *E. limosus* (**Figure 4**).

Phenotyping of *E. viscosium* and *E. limosus*:

To further understand the morphology, growth capabilities, and stress responses of *E. viscosium* and *E. limosus*, we performed multiple phenotyping experiments. The intent of these experiments was to provide a broader perspective on the potential adaptations that would support the ability of these fungi to successfully colonize biological soil crusts and other extreme niches.

Budding patterns

Due to these species' similarities in colony morphology, observations of budding patterns in these new species became an essential task for differentiation. Microscopy was initially performed on cells grown from solid agar plates, which provided us with basic information that their cell morphology was different, with *E. viscosium* being very round and yeast-shaped and *E. limosus* having more elongated, connected cells. But details regarding their budding patterns and cell polarity we're also needed. Using adapted protocols from (Mitchison-Field et al., 2019) we were able to perform a long-term microscopy time-lapse of the budding patterns of these species using the VALAP (1:1:1 Vasoline: Lanolin: Parafin) method to seal the edges of a coverslip while allowing gas exchange for cells to actively grow (**Figure 6**). From this we were able to observe dramatic differences in the budding types of *E. viscosium* and *E. limosus*. *E. viscosium* buds with round cells in initially a distal fashion where the new bud forms 180° from the mother cell origination site, but also forms new buds at a ~90° angle from where the mother bud was formed in a proximal manner (**Figure 5; Video 1**). *E. limosus* on the other hand forms elongated cells in a distal manner, forming longer chains of cells instead of clusters, with axial buds forming at later timepoints (**Figure 5; Video 2**). These morphological differences in budding patterns influences the way these two species grow in a shaking flask. For example, *E. limosus* forms more elongated cells and buds distally which while does not create true hyphae, still creates larger clumps of cells which are not easily pipetted. However, *E. viscosium* since it forms rounder cells and buds with both distal and proximal patterns, does not form extensive clumps in a shaking flask and is more easily pipetted. *E. limosus* also forms more extensive biofilms at the liquid-air interface than *E. viscosium*, likely also due to the elongated cell morphology.

Growth of E. viscosium and E. limosus on 8 different medias:

Growth of *E. viscosium* and *E. limosus* on a variety of different media was done to assess growth requirements and their impact on pigmentation (**Figure 6**). The media used are described in **Table 1**, and include MAG, MEA, MN+NAG, MNV, PDA, Spider, YPD, and V8. The addition of Vitamin mix (Table 1) to any medium, but specifically to MAG and MN, caused the growth of both isolates to become much shinier, blacker (vs. browner), and more yeast-like. Growth on MEA causes the formation of a rainbow sheen, which is not seen on any other medium. Spider medium and YPD caused the formation of a dark-colored halo around colonies of both species. However, the halo around colonies grown on YPD is much darker and extends further than on Spider medium, and *E. viscosium* showed a more extensive halo than *E. limosus*. The ability of both species to grow on V8 medium implies that they can use cellulosic material as a carbon source. Overall, colony growth and pigmentation were similar across of media types for both species (**Figure 6**).

Carbon and nitrogen utilization

Carbon source utilization was determined using Biomerieux C32 carbon strips, which are typically used for identification of human pathogens (Tragiannidis et al., 2012). Following the protocols provided by the vendor, we were able to show that *E. viscosium* and *E. limosus* can utilize a wide range of carbon sources. Triplicates were performed on these strips to ensure results were uniform and representative. Overall, a variety of carbon sources supported robust growth of both species (e.g., D-glucose, L-sorbose, D-galactose, N-acetyl glucosamine, D-sorbitol, D-xylose, glycerol, L-rhamnose, L-arabinose, D-celliobiose, and maltose), and there are only a few quantitative differences in utilization patterns (**Figure 7; Table 5**). Carbon sources that could not support growth include D-rafinose, D-melibiose, methyl-aD-glucopyranoside, and D-lactose. Both species were resistant to cycloheximide and were capable of

producing a black color in the presence of esculin ferric citrate (**Figure 7**). Notably, for both *E. viscosium* and *E. limosus*, growth on some carbon sources, particularly sorbose, levulinic acid, and N-acetyglucosamine, lead to enhanced pigmentation (**Figure 7**).

We were particularly interested in patterns of nitrogen utilization for *E. viscosium* and *E. limosus* given their isolation from a nutrient deplete niche with extensive nitrogen-fixing bacterial populations. Nine different nitrogen sources were tested: five amino acids (aspartate, glutamate, glycine, proline, serine), ammonium tartrate, sodium nitrate, urea, peptone (mixed short chain amino acids) as a positive control, and no nitrogen as a negative control. Both species are incapable of utilizing Aspartate and Glutamate as nitrogen sources (**Figure 8**). Preferred nitrogen sources for both species include ammonia and proline. However, they differ in that *E. viscosium* also prefers urea while *E. limosus* also prefers serine (**Figure 8**). Otherwise, patterns of nitrogen utilization appear generally similar across both species.

Optimal Growth Temperature and Range of growth temperatures

E. viscosium and *E. limosus* were isolated from an environment that experiences wide seasonal and diurnal temperature changes. As such, we wanted to determine both the optimal growing temperature for these species, as well as the limits at which they are capable of survival. Both isolates were serial diluted and spotted onto MEA plates to determine the carrying capacity at different temperatures. Both *E. viscosium and E. limosus* were capable of growth at 4 °C, 15 °C, 23 °C, and 27 °C, but could not grow at 37 °C and 42 °C (**Figure 9**). Optimal growth temperature of both *E. viscosium* and *E. limosus* was 23 °C (**Figure 9**). Growth at 4 °C was slow, but after a year the isolates both species formed extensive colonies and flooded the agar with melanin (**Figure 10**). Although neither species grew at 37 °C, they retained viability as they were able to resume growth following return to 23 °C after three days exposure to 37 °C (**Figure 10**). In contrast, a similar experiment showed that incubation at 42 °C is lethal.

UV and metal resistance

Melanized fungi are recognized for their resistance to UV light, and the possibility of using ionizing radiation as an energy source (Dadachova et al., 2007). To assess the response of *E. viscosium* and *E. limosus* to UV radiation, they were each exposed to a dose (120 seconds of 10,000 μJ/cm^2 at 254 nm) that was lethal to *S. cerevisiae* and *E. dermatitidis* (data not shown). The same level of exposure did not kill either *E. viscosium* or *E. limosus* (**Figure 11**) but did significantly reduce the number of viable colonies. Strikingly, surviving colonies showed no evidence of induced mutagenesis based on the absence of altered morphologies or pigmentation (**Figure 11**).

Polyextremotolerant fungi have been previously noted as having increased metal resistances as a result of their melanized cell wall and other adaptations to harsh environments (Gadd & de Rome, 1988). To test if these two new *Exophiala* spp. possess increased metal resistances when compared to *E. dermatitidis* and *S. cerevisiae*, we impregnated Whatman filter discs with various metals of different concentrations. Diameters of zones of clearing revealed no evidence for enhanced metal resistance in *E. viscosium* or *E. limosus* (**Table 6**). On the other hand, both species appear to be moderately more sensitive to $NiCl_2$ and $CdCl_2$ (**Table 6**).

Lipid Profiles

Both *E. viscosium* and *E. limosus* appear to possess abundant lipid bodies (**Figure 3**). This observation along with the unique sticky morphology of both species led us to the idea that they might contain

unique or copious amounts of lipids. We performed a Bligh and Dyer lipid extraction followed by thin layer chromatography (TLC) to observe patterns of lipid accumulation in *E. viscosium* and *E. limosus* grown on media that contained fermentable or non-fermentable sugars, both with high nitrogen and low nitrogen. These iterations creating four unique medias would allow us to cover as much of a spread of lipid changes as possible. S. *cerevisiae* and *E. dermatitidis* were also similarly analyzed. Results from this lipid extraction showed that our two new species did not seem to produce any unique or novel amounts or types of lipids when compared to *S. cerevisiae* and *E. dermatitidis* (**Figure 12**).

Melanin production and regulation in *E. viscosium* and *E. limosus*

Melanin biosynthesis gene annotation

A defining feature of black yeasts such as *E*. *viscosium* and *E*. *limosus* is their pigmentation caused by the accumulation of melanin (Bell & Wheeler, 1986). Given the presumed importance of melanin to a polyextremotolerant lifestyle, we are interested in understanding how melanin production is regulated in response to environmental inputs. A first step in this process is to determine the types of melanin that *E*. *viscosium* and *E*. *limosus* are capable of producing. To accomplish this, the sequenced genomes of *E. viscosium* and *E. limosus* were annotated using protein sequences for all three melanin biosynthetic pathways in *Aspergillus niger* (Teixeira et al., 2017). The list of *A. niger* genes and their homologs in both *E. viscosium* and *E. limosus* are summarized in **Table 7**. Manual annotation and reverse BLASTP of the melanin biosynthesis pathway genes showed that both *E. viscosium* and *E. limosus* have the genetic capability to produce all three forms of known fungal melanins: DOPA melanin (pheomelanin), DHN melanin (allomelanin), and L-tyrosine derived pyomelanin.

Regulation of Melanin production using chemical blockers

Because *E*. *viscosium* and *E*. *limosus* possess the capability to produce all three forms of fungal melanin, we asked whether they were all being produced simultaneously or if one was preferred for production versus secretion. We used chemical blockers for both DOPA melanin and DHN melanin to determine the predominant type of melanin produced on MEA and YPD. Kojic acid blocks the production of DOPA melanin, whereas Phthalide inhibits the synthesis of DHN melanin; both are effective at doses of 1, 10, and 100 µg/mL (Pal et al., 2014).

First, we used 100 mM of phthalide and 100 mg/mL of kojic acid in a filter dick assay. Placing drug-impregnated filter discs on freshly spread lawns of cells either individually or with both drugs combined did not block melanin production even though the concentrations of the drugs were higher than that of previous studies (**Figure 13**). Then using Pal et al.'s method of melanin blocking (Pal et al., 2014), we added the highest dosage (100 µg/mL) of Phthalide and Kojic acid individually and combined to agar-solidified MEA, and both spread a lawn of cells and spotted serially diluted cells onto the plates. Neither assay resulted in blockage of melanin production in *E. viscosium* or *E. limosus* (**Figure 13**). However, addition of 100 µg/mL of Phthalide alone did result in their apparent secretion of a dark substance into MEA (**Figure 14**). Overall, chemical inhibition of DOPA melanin or DHN melanin production did not qualitatively reduce colony pigmentation, possibly suggesting that the tyrosine-derived pyomelanin is still being produced.

Melanin Secretion

The appearance of a dark pigment surrounding colonies of *E*. *viscosium* and *E*. *limosus* under specific conditions raised the idea that these yeasts are able to secrete melanin into their local environment. The presence of dark pigments in the supernatants of liquid cultures lent further support to this.

Initial studies were performed to determine which media triggered the release of melanin. Both *E. viscosium* and *E. limosus* were capable of releasing the most melanin and in the shortest growth time on YPD, with *E. viscosium* seemingly secreting more than *E. limosus* (**Figure 5**). Because YPD and MEA only differ in yeast vs. malt extract as well as the percentage of peptone (2% in YPD, 0.2% in MEA), we first determined if the peptone differences impacted melanin secretion. By switching the peptone amounts in YPD and MEA, we demonstrated that *E. viscosium* acquired the ability to secrete melanin on MEA if it was supplemented with 2% peptone. To extend this observation, we added progressively higher amounts of peptone to MEA media (i.e., 10 different concentrations of peptone ranging from 0.1% to 5%). We observed that *E. viscosium* starts secreting melanin on MEA at a peptone amount of 2%, and *E. limosus* starts secreting melanin at about 4% peptone (**Figure 16**).

Confirmation of active melanin secretion from living cells

To confirm that the dark pigment in culture supernatants is indeed melanin, we performed a melanin extraction using previously described methods (Pal et al., 2014; Pralea et al., 2019). Although both enzymatic and chemical extraction of melanin was attempted, the chemical extraction process proved to be more efficient at recovering secreted melanin (**Figure 17**). Therefore, all extractions going forward were performed using the chemical extraction method to ensure all melanin was precipitated out of the solution.

Growth of *E. viscosium, E. limosus,* and *E. dermatitidis* on YPD and MEA were observed daily for melanin secretion; 11 mL aliquots of their supernatant were removed daily, and the melanin was extracted from each sample. As the experiment progressed, it was obvious that *E. viscosium* and *E. limosus* began secreting melanin on day 3 and secreted more in YPD than in MEA (**Figure 18**). *E. dermatitidis* on the other hand seemed to have a slower build-up of melanin, and melanin wasn't truly obvious in the medium until day 6 in MEA though it can be seen in MEA day 3 in **Figure 18**. Analysis of the optical density (OD) of extracted melanin revealed that melanin amount increased over the course of the experiment, and that greater amounts of melanin are released in YPD for *E. viscosium* and *E. limosus* compared to MEA for *E. dermatitidis* (**Figure 17**). Interestingly, for both *E. viscosium* and *E. limosus*, their peak melanin secretion was on day 6 and not on day 7 (**Figure 19**). There was actually less melanin on day 7 for both species, indicating that the melanin after day 6 was either degrading, or was being taken back up by the cells. This was only obvious with reading the OD results of the extracted melanin, as the supernatants themselves day 5 and on were all strikingly dark and hard to differentiate visually (**Figure 18**). Extracted melanin from all *E. viscosium* and *E. limosus* samples displayed the typical results from a full spectrum read on pure melanin, *E. dermatitidis* did not show typical melanin spectrum results until day 6 in YPD but were typical every day in MEA. When graphed with OD to Wavelength the sample should have an exponentially decreasing OD as wavelength increases, and when the OD is changed to a log scale, the full spectrum read should be a linear regression with an R^2 value of 0.97 or higher (Pralea et al., 2019). All *E. viscosium* and *E. limosus* samples displayed these features, and therefore we can confirm that the dark nature of their supernatants is caused by actively secreted melanin.

Genetic analysis of Melanin Production

Recovery of an albino mutant

At this time, molecular tools for the manipulation of *E. viscosium* and *E. limosus* are not yet available. Therefore, we combined classical genetics with genome re-sequencing to initially investigate the regulation of melanin production. Following mutagenesis with the alkylating agent ethyl methyl sulfonate (EMS), mutants following into four distinct phenotypic classes were recovered: pink/albino, crusty, brown, and melanin over-secretion (Data not shown). The most intriguing of these phenotypes was the pink/albino phenotype found in a mutant of *E. limosus* we called EMS 2-11 (**Figure 20**). This mutant is considered albino but colored pink likely due to *Exophiala* spp. production of carotenoids. It has already been shown that blockage of melanin production in *E. dermatitidis* by mutations in *pks1* results in pink instead of white albino colonies because they also produce carotenoids and by-products such as flavolin that are normally masked by melanin (Geis & Szaniszlo, 1984; Geis et al., 1984).

Genome re-sequencing of high molecular weight DNA from mutant EMS 2-11 and comparison to the reference *E. limosus* genome revealed a deleterious SNP causing a nonsense mutation in *pks1*. This mutation was on position 2,346,590 in scaffold 3, located in the *pks1* gene, which caused an C -> T mutation on the first position of the codon such that it became a stop codon. Interestingly, *pks1* only functions in one of the three melanin biosynthetic pathways found in *E. limosus*. Only two of the other random mutations found in EMS 2-11 were missense or nonsense mutations. One is a mutation in a transcriptional repressor EZH1, and another is in alcohol dehydrogenase GroES-like/Polyketide synthase enolreductase. Although either of these mutations could contribute to the pink phenotype, it is more likely that a nonsense mutation in *pks1* is solely responsible for the loss of melanin production despite the lack of mutations in the other melanin biosynthetic pathways.

Recovery of melanin production in albino mutant

Pks1 is a polyketide synthase that is essential for the first step in the DHN-melanin/Allomelanin production pathway. To test if “activation” of an alternative melanin production pathway could restore melanin production to the EMS 2-11 mutant, we substituted 1 mM of L-DOPA into the medium. As L-DOPA was shown to recover melanization in a *pks1* deletion mutant of *E. dermatitidis*, thus presumed that it would be taken up by our EMS 2-11 mutant and activate the DOPA melanin/pheomelanin biosynthesis pathway (Dadachova et al., 2007; Paolo et al., 2006). However, substitution of 1 mM L-DOPA into either MEA or YPD did not induce melanin production in the EMS 2-11 *pks1* mutant (**Figure 20**). These plates were grown in the dark for 10 days, as L-DOPA will auto polymerize into a melanin precursor in the presence of light, and still no melanin production was observed. Hydroxyurea is another compound that in other *Exophiala* species induces melanin production, however addition of 20 mM of Hydroxyurea also did not activate melanin production in our EMS 2-11 albino mutant (**Figure 20**) (Schultzhaus et al., 2020). Finally, we substituted in 1 mM of 1,8-DHN into their media which is the immediate precursor to DHN melanin, in hopes of recovering the expected melanin biosynthetic process with a *pks1* mutant. This did result in recovery of melanized colonies, while on MEA they do not form extensive growth, their cells are still dark, and on YPD active dark colony growth is observed (**Figure 20**).

Discussion

A major limitation to our understanding of the roles played by BSCs in semi-arid ecosystems is our lack of insight into the microbial components of these biofilms and the nature of their functional interactions (Carr et al., 2021). As photoautotrophs, the roles of cyanobacteria and algae in BSCs are clear (Belnap, 2002), but the importance of other residents such as fungi and bacteria is less so. Here, we identify two novel species of black yeasts from BSCs; *E. viscosium* and *E. limosus*. In addition to presenting the complete annotated genome sequence for each species, we also provide a relatively detailed profile of their ability to utilize diverse carbon and nitrogen sources, as well as their response to different forms of stress. Most importantly, we demonstrate that *E. viscosium* and *E. limosus* are capable of producing excessive amounts of melanin, including melanin that is secreted at high levels. Our results suggest that by making melanin available as a public good, black yeasts provide a critical service to the broader BSC community.

Description and genome features of E. viscosium and E. limosus

E. viscosium and *E. limosus* are two novel fungi from the family Herpotrichielleaceae that we isolated from a lichen-dominated BSC. Distinguishing features of these isolates includes their yeast morphology, pronounced melanization, and production of extracellular material that leads to the formation of "goopy" or "slimy" colonies. Notably, numerous other melanized fungi with filamentous or polymorphic characteristics were isolated from the same BSC communities. These fungi, which will be described in detail elsewhere, grow much more slowly than *E. viscosium* or *E. limosus* and also release much less melanin. Phylogenetic comparisons suggest that the closest relative of *E. viscosium* and *E. limosus* is *E. sideris*. Comparison of their respective annotated genome sequences revealed that overall gene content and characteristics are similar across all three species. *E. sideris* belongs to the *jeanselmei*-clade of *Exophiala* species; it is typically recovered from highly polluted environments and is not known to be pathogenic (Seyedmousavi et al., 2011). The failure of *E. viscosium* and *E. limosus* to grow at 37 ^{o}C reinforces the point that species within this clade are less likely to possess the capacity of causing disease in mammals. One interesting feature that the genome comparisons of *E. sideris* to *E. viscosium* and *E. limosus* revealed was that *E. sideris* contains a lower predicted gene content than the other two isolates. This could be a factor of their differences in their ecology and lifestyles. *E. sideris* was isolated from a highly toxic environment containing arsenate, hydrocarbons, and other toxins meaning this species had to specialize in withstanding these toxins rather than generalizing its survival genetic toolbox (Seyedmousavi et al., 2011). MAT organization of the MAT locus between these homothallic species is very similar, all containing a fused *MAT* gene, with the exception of different transcript directionality for the flanking *cox13* and *apc5* genes. Many *Exophiala* species are indicated to be heterothallic, even closely related species to *E. sideris* such as *E. oligosperma* and *E. spinifera* are heterothallic (Teixeira et al., 2017; Untereiner & Naveau, 1999). Whereas *E. sideris* itself and now *E. viscosium* and *E. limosus* all contain a fused or cryptic MAT gene which has been hypothesized to cause homothallism as a result of a parasexual cycle that occurred (Teixeira et al., 2017). Further investigation of these ideas will require demonstration that these *Exophiala* species undergo sexual development.

Phenotypic characterization of E. viscosium and E. limosus

Our results show that *E. viscosium* and *E. limosus* are capable of using a diverse array of carbon sources. These include mannitol, ribitol, and glucose, which are considered the main carbon sources exchanged between photobionts and their mycobiont partners in lichens (Richardson et al., 1967; Yoshino et al., 2020). Although, *E. viscosium* and *E. limosus* are able to use most nitrogen sources provided, glutamate

and aspartate are clearly not being taken up or used, unlike in yeasts such as *S. cerevisiae* where glutamate is a more favorable nitrogen source used for multiple core metabolism and amino acid production processes (Ljungdahl & Daignan-Fornier, 2012). Because peptone is a favorable nitrogen source for *E. viscosium* and *E. limosus*, it is likely that these species can import peptides and degrade them as sources of ammonia. Their preferred nitrogen source is ammonium/ammonia though, which in their ecological environment would likely be produced by cyanobacteria and other nitrogen-fixing bacteria (Belnap, 2002). However, they can also use nitrate and urea as nitrogen sources, again pointing to their metabolic flexibility in their nutrient deplete ecosystem.

A characteristic feature of BSCs is the inherently stressful nature of these ecosystems. Of note, *E. viscosium* and *E. limosus* were isolated from a site that can experience extremes in temperature, UV exposure, and soil wetness/osmotic pressure. Although the optimal growth range for these species is from 15 °C to 27 °C, they are capable of slow growth at 4 °C and while they do not grow at 37 °C, they do remain viable after 72 consecutive hours of exposure to this temperature. The ability to grow at 4°C, albeit slowly, presumably contributes to the success of fungi such *E. viscosium* and *E. limosus* in adapting to BSCs in colder drylands. A broader comparison of microbiomes and associated functional traits between cold-adapted BSCs and those found in hot deserts would be an informative approach to identifying microbial species and/or physiological factors that underlie temperature adaptation.

As for resistance to UV radiation, *E. viscosium* and *E. limosus* were both able to survive the high exposure of UV-C that was used and were uniquely resistant to standard UV mutagenesis conditions. Potential mechanisms that might contribute to UV resistance include the presence of melanin or other defensive compounds, some of which could be public goods provided by other constituents of the BSC community, or an enhanced capacity to repair damaged DNA. This will ultimately be an interesting topic to investigate in the future.

One feature we expected to find in *E. viscosium* and *E. limosus* but we did not necessarily observe was higher metal resistance. Melanin is known to enhance resistances to metals (Bell & Wheeler, 1986; Gadd, 1994; Gorbushina, 2007; Purvis et al., 2004), and so we predicted that these species would have increased metal tolerance when compared to non-melanized fungi. However, of the metals tested, only $AgNO_3$ and $CuCl_2$ showed a decreased zone of clearing in *E. viscosium* and *E. limosus*, compared to *S. cerevisiae* and *E. dermatitidis*. A potential explanation for the latter observation is that melanin has a higher affinity for copper due to the phenolic compounds within the polymer (Gadd & de Rome, 1988).

Secretion of melanin by E. viscosium and E. limosus

Melanin is considered an expensive secondary metabolite to produce because it is made up of conglomerates of polyphenols and as such contains many carbons (Schroeder et al., 2020). Therefore, it would be assumed that an organism would not want to create melanin just to export it out of the cell unless there was a beneficial reason behind it. Additionally, there are not many fungi known to secrete melanin and few in the genus *Exophiala*, so the possibility of novel species that secrete melanin into their surroundings was intriguing. Both novel fungi have the genetic makeup to produce all three types of fungal melanin: allomelanin (DHN derived), pyomelanin (L-tyrosine derived), and pheomelanin (L-DOPA derived); but it is still unknown how these melanin biosynthetic pathways are regulated, and which are being actively produced.

In our attempts to understand the regulation of melanin production by *E. viscosium* and *E. limosus* we tried blocking individual pathways using known chemical blockers of DHN and DOPA melanin, phthalide and kojic acid respectively. Neither blocker, nor their combination at the highest amounts used were able to block the production of melanin in either species. If these species have the capability to produce all three melanins, then it is possible that they are producing more than one at the same time. This could be the case here, since the combination of both kojic acid and phthalide still resulted in melanized cells which would indicate that tyrosine-derived pyomelanin was the cause of melanization.

Linked regulation of potentially multiple forms of melanin was observed with our EMS-induced mutant in which the *pks1* gene contained a nonsense mutation. Although *pks1* is the first enzyme involved in only the production of DHN-derived allomelanin, the cells that resulted from this mutation were albino. Theoretically, these cells should have still been capable of producing the two other melanins as their pathways were seemingly not disrupted by any mutations, but this was not the case. Addition of L-DOPA has been shown to induce melanization in a *pks1* deletion mutant of *E. dermatitidis* (Paolo et al., 2006), which would indicate that it is capable of producing both pheomelanin and allomelanin. However, the same experiment performed on *E. limosus*' *pks1* nonsense mutant did not recover melanization. Therefore, it is possible that; (i) *E. viscosium* and *E. limosus* only produce DHN-derived allomelanin and disruption of *pks1* causes all melanin production to shut down, (ii) *pks1* (or downstream creation of allomelanin) is essential for the regulation of other melanin productions, or (iii) pheomelanin and pyomelanin are only produced under specific conditions that were not used during analysis of the mutants.

Our experiments also showed that *E. viscosium* and *E. limosus* actively secrete melanin when they are viable and growing. We observed that melanin began to accumulate starting as early as day 2, therefore suggesting live cells are secreting melanin and not leaked from dead lysed cells. We also observed a decrease in melanin concentrations after day 6 in both YPD and MEA, which raises the intriguing potential for melanin uptake or degradation by *E. viscosium* and *E. limosus*.

The medium that stimulated the most melanin secretion is YPD which has 10x more nitrogen (2% vs. 0.2%) than the alternative medium we use, MEA, which neither fungus secrete melanin into when plated on solid media. This led us to believe that nitrogen amount could potentially have an effect on the production of secreted melanin, which we did observe as we increased peptone amounts in the medium. Interestingly, the only fungal melanin that has nitrogen in its precursor structure is the DOPA derived pheomelanin. This was one of two melanins that could be produced in the presence of phthalide, which we observed also induced the secretion of melanin in these fungi. This provides support that the secreted melanin is either pheomelanin, as it requires more nitrogen in order to be produced, or that the production of pheomelanin (DOPA) and the water soluble pyomelanin (Turick et al., 2010) are linked.

Insights into the niche of polyextremotolerant fungi within the biological soil crust consortium

Fungal residents of BSC communities include lichenized mycobionts, lichenicolous fungi, endolichenic fungi, and free-living fungi. Although the latter are likely not directly associated with lichens themselves, they are surrounded by algae, cyanobacteria, and other bacteria in the same way that lichen-associated fungi are surrounded by a similar community of microbes. This raises the intriguing possibility that fungi such as *E. viscosium* and *E. limosus* might transiently associated with phototrophs in response to specific environmental conditions. Members of the genus *Exophiala* (Class Eurotiomycetes) are phylogenetically

related to the lichen-forming Verrucariales, and reside between Lecanoromycetes and Lichinomycetes (James et al., 2006). Additionally, lifestyle changes within Eurotiomycetes contributed to the polyphyletic nature of lichenization within the Ascomycetes, but since surrounding taxa are lichenized it is more likely that these species lost lichenization than three distinct lichenization events occurring within closely related species (Lutzoni et al., 2001). Because *E. viscosium* and *E. limosus* have lichenized ancestors, they could conceivably have lost their "true lichenization" capabilities, but maintained the genetic tools to interact with algae, cyanobacteria, and other bacteria to form lichen-like symbioses. As these are two newly identified species, more extensive ecological and molecular investigation is needed to determine the extent to which these taxa are found in BSCs and to elucidate their species interaction networks.

Correlation between environmental nitrogen availability and secreted melanin amounts could have strong implications for interactions between these fungi found in BSCs and their nitrogen-fixing community partners. The presumed source of nitrogen used to enhance the secretion of melanin would be from nitrogen-fixing prokaryotes such as cyanobacteria, other bacteria, and archaea in the community. Our results suggest that the availability of these nitrogen-fixers to provide fungal cells with ammonia could subsequently induce the secretion of melanin that then provides protective services to the broader BSC community. Secreted melanin could function at the community-level to maintain respiration and growth under varying temperature conditions while also mitigating the effects of desiccation and exposure to UV, extending the window of time allotted for optimal photosynthetic capabilities (Carr et al., 2021; Honegger, 1997; Honegger & Haisch, 2001; Lange & Tenhunen, 1981; Nybakken et al., 2004). Moreover, the secreted melanin could simultaneously serve as an external source of carbon used by the fungi and possibly others when the environment does not allow for photosynthesis. In either scenario, the seemingly wasteful secretion of melanin by *E. viscosium* and *E. limosus* instead represents the optimal sharing of an expensive public good for the overall betterment of the BSC community in which they reside.

The availability of complete, annotated genome sequences for *E*. *viscosium* and *E. limosus* will enable more detailed investigations of the mechanisms that support the adaptation of these fungi to extreme environments. This in turn should provide greater insight into the roles that these fungi play in the BSC community. Of particular interest will be the regulatory mechanisms that coordinate the production of different types of melanin in response to environmental and chemical inputs. Moreover, the broad applicability of melanin as a bioproduct has triggered growing interest in microorganisms that secrete this polymer. In this context, *E*. *viscosium* and *E. limosus* could potentially serve as excellent platforms for additional engineering focused on optimizing or tailoring the type of melanin produced in responses to specific applications.

Acknowledgements

The authors would like to acknowledge Dr. Rajib Saha for providing a pre-print review of this work, with his guidance we were able to make this manuscript as clear and concise as possible. The work (proposal: 10.46936/10.25585/60001081) conducted by the U.S. Department of Energy Joint Genome Institute, a DOE Office of Science User Facility, is supported by the Office of Science of the U.S. Department of Energy under Contract No. DE-AC02-05CH11231. Funding for this work was provided by NASA grant number 80NSSC17K0737.

941

942 Citations:

943 Ametrano, C. G., Selbmann, L., & Muggia, L. (2017). A standardized approach for co-culturing
944 Dothidealean rock-inhabiting fungi and lichen photobionts in vitro. *Symbiosis*, *73*(1), 35-44.
945 Bates, S. T., Garcia-Pichel, F., & Nash III, T. (2010). Fungal components of biological soil crusts: insights
946 from culture-dependent and culture-independent studies. *Bibliotheca Lichenologica*, *105*, 197-
947 210.
948 Bates, S. T., Reddy, G. S., & Garcia-Pichel, F. (2006). Exophiala crusticola anam. nov.(affinity
949 Herpotrichiellaceae), a novel black yeast from biological soil crusts in the Western United States.
950 *International journal of systematic and evolutionary microbiology*, *56*(11), 2697-2702.
951 Bell, A. A., & Wheeler, M. H. (1986). Biosynthesis and functions of fungal melanins. *Annual review of*
952 *phytopathology*, *24*(1), 411-451.
953 Belnap, J. (2002). Nitrogen fixation in biological soil crusts from southeast Utah, USA. *Biology and*
954 *fertility of soils*, *35*(2), 128-135.
955 Belnap, J. (2003). The world at your feet: desert biological soil crusts. *Frontiers in Ecology and the*
956 *Environment*, *1*(4), 181-189.
957 Belnap, J., Büdel, B., & Lange, O. L. (2001). Biological soil crusts: characteristics and distribution. In
958 *Biological soil crusts: structure, function, and management* (pp. 3-30). Springer.
959 Belnap, J., & Eldridge, D. (2001). Disturbance and recovery of biological soil crusts. In *Biological soil*
960 *crusts: structure, function, and management* (pp. 363-383). Springer.
961 Belnap, J., & Lange, O. L. (2003). *Biological soil crusts: structure, function, and management* (Vol. 150).
962 Springer.
963 Bligh, E. G., & Dyer, W. J. (1959). A rapid method of total lipid extraction and purification. *Canadian*
964 *journal of biochemistry and physiology*, *37*(8), 911-917.
965 Bowker, M. A., Reed, S., Belnap, J., & Phillips, S. (2002). Temporal variation in community composition,
966 pigmentation, and Fv/Fm of desert cyanobacterial soil crusts. *Microbial Ecology*, 13-25.
967 Bowker, M. A., Soliveres, S., & Maestre, F. T. (2010). Competition increases with abiotic stress and
968 regulates the diversity of biological soil crusts. *Journal of Ecology*, *98*(3), 551-560.
969 Cao, W., Zhou, X., McCallum, N. C., Hu, Z., Ni, Q. Z., Kapoor, U., . . . Mantanona, A. J. (2021). Unraveling
970 the structure and function of melanin through synthesis. *Journal of the American Chemical*
971 *Society*, *143*(7), 2622-2637.
972 Carr, E. C., Harris, S. D., Herr, J. R., & Riekhof, W. R. (2021). Lichens and biofilms: Common collective
973 growth imparts similar developmental strategies. *Algal Research*, *54*, 102217.
974 Castresana, J. (2000). Selection of conserved blocks from multiple alignments for their use in
975 phylogenetic analysis. *Molecular biology and evolution*, *17*(4), 540-552.
976 Cordero, R. J., & Casadevall, A. (2017). Functions of fungal melanin beyond virulence. *Fungal Biology*
977 *Reviews*, *31*(2), 99-112.
978 Cubero, O. F., Crespo, A., Fatehi, J., & Bridge, P. D. (1999). DNA extraction and PCR amplification method
979 suitable for fresh, herbarium-stored, lichenized, and other fungi. *Plant Systematics and*
980 *Evolution*, *216*(3), 243-249.
981 Dadachova, E., Bryan, R. A., Huang, X., Moadel, T., Schweitzer, A. D., Aisen, P., . . . Casadevall, A. (2007).
982 Ionizing radiation changes the electronic properties of melanin and enhances the growth of
983 melanized fungi. *PloS one*, *2*(5), e457.
984 De Hoog, G., Vicente, V., Caligiorne, R., Kantarcioglu, S., Tintelnot, K., Gerrits van den Ende, A., & Haase,
985 G. (2003). Species diversity and polymorphism in the Exophiala spinifera clade containing
986 opportunistic black yeast-like fungi. *Journal of Clinical Microbiology*, *41*(10), 4767-4778.

Donlan, R. M., & Costerton, J. W. (2002). Biofilms: survival mechanisms of clinically relevant microorganisms. *Clinical microbiology reviews*, *15*(2), 167-193.

Frases, S., Salazar, A., Dadachova, E., & Casadevall, A. (2007). Cryptococcus neoformans can utilize the bacterial melanin precursor homogentisic acid for fungal melanogenesis. *Applied and environmental microbiology*, *73*(2), 615-621.

Gadd, G. M. (1994). Interactions of fungi with toxic metals. *The Genus Aspergillus*, 361-374.

Gadd, G. M., & de Rome, L. (1988). Biosorption of copper by fungal melanin. *Applied microbiology and biotechnology*, *29*(6), 610-617.

Geis, P. A., & Szaniszlo, P. J. (1984). Carotenoid pigments of the dematiaceous fungus Wangiella dermatitidis. *Mycologia*, *76*(2), 268-273.

Geis, P. A., Wheeler, M. H., & Szaniszlo, P. J. (1984). Pentaketide metabolites of melanin synthesis in the dematiaceous fungus Wangiella dermatitidis. *Archives of microbiology*, *137*(4), 324-328.

Gessler, N., Egorova, A., & Belozerskaya, T. (2014). Melanin pigments of fungi under extreme environmental conditions. *Applied Biochemistry and Microbiology*, *50*(2), 105-113.

Gnerre, S., MacCallum, I., Przybylski, D., Ribeiro, F. J., Burton, J. N., Walker, B. J., . . . Jaffe, D. B. (2011). High-quality draft assemblies of mammalian genomes from massively parallel sequence data. *Proceedings of the National Academy of Sciences*, *108*(4), 1513-1518. https://doi.org/10.1073/pnas.1017351108

Gorbushina, A. A. (2007). Life on the rocks. *Environmental microbiology*, *9*(7), 1613-1631.

Gostinčar, C., Grube, M., De Hoog, S., Zalar, P., & Gunde-Cimerman, N. (2009). Extremotolerance in fungi: evolution on the edge. *FEMS microbiology ecology*, *71*(1), 2-11.

Gostinčar, C., Grube, M., & Gunde-Cimerman, N. (2011). Evolution of fungal pathogens in domestic environments? *Fungal biology*, *115*(10), 1008-1018.

Gostinčar, C., Muggia, L., & Grube, M. (2012). Polyextremotolerant black fungi: oligotrophism, adaptive potential, and a link to lichen symbioses. *Frontiers in Microbiology*, *3*, 390.

Grabherr, M. G., Haas, B. J., Yassour, M., Levin, J. Z., Thompson, D. A., Amit, I., . . . Zeng, Q. (2011). Full-length transcriptome assembly from RNA-Seq data without a reference genome. *Nature biotechnology*, *29*(7), 644-652.

Grigoriev, I. V., Nikitin, R., Haridas, S., Kuo, A., Ohm, R., Otillar, R., . . . Shabalov, I. (2014). MycoCosm portal: gearing up for 1000 fungal genomes. *Nucleic Acids Research*, *42*(D1), D699-D704. https://doi.org/10.1093/nar/gkt1183

Grube, M., Cernava, T., Soh, J., Fuchs, S., Aschenbrenner, I., Lassek, C., . . . Sensen, C. W. (2015). Exploring functional contexts of symbiotic sustain within lichen-associated bacteria by comparative omics. *The ISME journal*, *9*(2), 412-424.

Hom, E. F., & Murray, A. W. (2014). Niche engineering demonstrates a latent capacity for fungal-algal mutualism. *Science*, *345*(6192), 94-98.

Honegger, R. (1997). Metabolic interactions at the mycobiont-photobiont interface in lichens. In *Plant relationships* (pp. 209-221). Springer.

Honegger, R., & Haisch, A. (2001). Immunocytochemical location of the (1→ 3)(1→ 4)-β-glucan lichenin in the lichen-forming ascomycete Cetraria islandica (Icelandic moss). *New phytologist*, *150*(3), 739-746.

James, T. Y., Kauff, F., Schoch, C. L., Matheny, P. B., Hofstetter, V., Cox, C. J., . . . Miadlikowska, J. (2006). Reconstructing the early evolution of Fungi using a six-gene phylogeny. *Nature*, *443*(7113), 818-822.

Katoh, K., Misawa, K., Kuma, K. i., & Miyata, T. (2002). MAFFT: a novel method for rapid multiple sequence alignment based on fast Fourier transform. *Nucleic acids research*, *30*(14), 3059-3066.

1033 Kobayashi, N., Muramatsu, T., Yamashina, Y., Shirai, T., Ohnishi, T., & Mori, T. (1993). Melanin reduces
1034 ultraviolet-induced DNA damage formation and killing rate in cultured human melanoma cells.
1035 *Journal of investigative dermatology*, *101*(5), 685-689.
1036 Kuo, A., Bushnell, B., & Grigoriev, I. V. (2014). Fungal genomics: sequencing and annotation. *Advances in*
1037 *Botanical Research*, *70*, 1-52.
1038 Lan, S., Wu, L., Zhang, D., & Hu, C. (2012). Successional stages of biological soil crusts and their
1039 microstructure variability in Shapotou region (China). *Environmental Earth Sciences*, *65*(1), 77-
1040 88.
1041 Lange, O., & Tenhunen, J. (1981). Moisture content and CO2 exchange of lichens. II. Depression of net
1042 photosynthesis in Ramalina maciformis at high water content is caused by increased thallus
1043 carbon dioxide diffusion resistance. *Oecologia*, *51*(3), 426-429.
1044 Letunic, I., & Bork, P. (2021). Interactive Tree Of Life (iTOL) v5: an online tool for phylogenetic tree
1045 display and annotation. *Nucleic acids research*, *49*(W1), W293-W296.
1046 Ljungdahl, P. O., & Daignan-Fornier, B. (2012). Regulation of amino acid, nucleotide, and phosphate
1047 metabolism in Saccharomyces cerevisiae. *Genetics*, *190*(3), 885-929.
1048 Lutzoni, F., Pagel, M., & Reeb, V. (2001). Major fungal lineages are derived from lichen symbiotic
1049 ancestors. *Nature*, *411*(6840), 937-940.
1050 Maier, S., Muggia, L., Kuske, C. R., & Grube, M. (2016). Bacteria and non-lichenized fungi within
1051 biological soil crusts. In *Biological Soil Crusts: An Organizing Principle in Drylands* (pp. 81-100).
1052 Springer.
1053 McFarland, J. (1907). The nephelometer: an instrument for estimating the number of bacteria in
1054 suspensions used for calculating the opsonic index and for vaccines. *Journal of the American*
1055 *Medical Association*, *49*(14), 1176-1178.
1056 Mitchison-Field, L. M. Y., Vargas-Muñiz, J. M., Stormo, B. M., Vogt, E. J. D., Van Dierdonck, S., Pelletier, J.
1057 F., . . . Gladfelter, A. S. (2019). Unconventional Cell Division Cycles from Marine-Derived Yeasts.
1058 *Current Biology*, *29*(20), 3439-3456.e3435. https://doi.org/10.1016/j.cub.2019.08.050
1059 Molina, L., & Molina, M. (1986). Absolute absorption cross sections of ozone in the 185-to 350-nm
1060 wavelength range. *Journal of Geophysical Research: Atmospheres*, *91*(D13), 14501-14508.
1061 Nybakken, L., Solhaug, K. A., Bilger, W., & Gauslaa, Y. (2004). The lichens Xanthoria elegans and Cetraria
1062 islandica maintain a high protection against UV-B radiation in Arctic habitats. *Oecologia*, *140*(2),
1063 211-216.
1064 Pal, A. K., Gajjar, D. U., & Vasavada, A. R. (2014). DOPA and DHN pathway orchestrate melanin synthesis
1065 in Aspergillus species. *Medical mycology*, *52*(1), 10-18.
1066 Paolo, W. F., Dadachova, E., Mandal, P., Casadevall, A., Szaniszlo, P. J., & Nosanchuk, J. D. (2006). Effects
1067 of disrupting the polyketide synthase gene WdPKS1 in Wangiella [Exophiala] dermatitidis on
1068 melanin production and resistance to killing by antifungal compounds, enzymatic degradation,
1069 and extremes in temperature. *BMC microbiology*, *6*(1), 1-16.
1070 Perez-Cuesta, U., Aparicio-Fernandez, L., Guruceaga, X., Martin-Souto, L., Abad-Diaz-de-Cerio, A.,
1071 Antoran, A., . . . Rementeria, A. (2020). Melanin and pyomelanin in Aspergillus fumigatus: from
1072 its genetics to host interaction. *International Microbiology*, *23*(1), 55-63.
1073 Pralea, I.-E., Moldovan, R.-C., Petrache, A.-M., Ilieș, M., Hegheș, S.-C., Ielciu, I., . . . Radu, M. (2019). From
1074 extraction to advanced analytical methods: The challenges of melanin analysis. *International*
1075 *journal of molecular sciences*, *20*(16), 3943.
1076 Price, M. N., Dehal, P. S., & Arkin, A. P. (2009). FastTree: computing large minimum evolution trees with
1077 profiles instead of a distance matrix. *Molecular biology and evolution*, *26*(7), 1641-1650.
1078 Purvis, O. W., Bailey, E. H., McLean, J., Kasama, T., & Williamson, B. J. (2004). Uranium biosorption by
1079 the lichen Trapelia involuta at a uranium mine. *Geomicrobiology Journal*, *21*(3), 159-167.

Pócs, T. (2009). Cyanobacterial crust types, as strategies for survival in extreme habitats. *Acta Botanica Hungarica*, *51*(1-2), 147-178.

Płonka, P., & Grabacka, M. (2006). Melanin synthesis in microorganisms: biotechnological and medical aspects. *Acta Biochimica Polonica*, *53*(3).

Rajeev, L., Da Rocha, U. N., Klitgord, N., Luning, E. G., Fortney, J., Axen, S. D., . . . Kerfeld, C. A. (2013). Dynamic cyanobacterial response to hydration and dehydration in a desert biological soil crust. *The ISME journal*, *7*(11), 2178-2191.

Richardson, D., Smith, D., & Lewis, D. (1967). Carbohydrate movement between the symbionts of lichens. *Nature*, *214*(5091), 879-882.

Rosas, Á. L., Nosanchuk, J. D., Gómez, B. L., Edens, W. A., Henson, J. M., & Casadevall, A. (2000). Isolation and serological analyses of fungal melanins. *Journal of immunological methods*, *244*(1-2), 69-80.

Schreier, W. J., Gilch, P., & Zinth, W. (2015). Early events of DNA photodamage. *Annual review of physical chemistry*, *66*, 497-519.

Schroeder, W. L., Harris, S. D., & Saha, R. (2020). Computation-driven analysis of model polyextremo-tolerant fungus exophiala dermatitidis: defensive pigment metabolic costs and human applications. *IScience*, *23*(4), 100980.

Schultzhaus, Z., Romsdahl, J., Chen, A., Tschirhart, T., Kim, S., Leary, D., & Wang, Z. (2020). The response of the melanized yeast Exophiala dermatitidis to gamma radiation exposure. *Environmental microbiology*, *22*(4), 1310-1326.

Seyedmousavi, S., Badali, H., Chlebicki, A., Zhao, J., Prenafeta-Boldu, F. X., & De Hoog, G. S. (2011). Exophiala sideris, a novel black yeast isolated from environments polluted with toxic alkyl benzenes and arsenic. *Fungal biology*, *115*(10), 1030-1037.

Teixeira, M. d. M., Moreno, L. F., Stielow, B., Muszewska, A., Hainaut, M., Gonzaga, L., . . . Souza, R. (2017). Exploring the genomic diversity of black yeasts and relatives (Chaetothyriales, Ascomycota). *Studies in mycology*, *86*, 1-28.

Tragiannidis, A., Fegeler, W., Rellensmann, G., Debus, V., Müller, V., Hoernig-Franz, I., . . . Groll, A. (2012). Candidaemia in a European Paediatric University Hospital: a 10-year observational study. *Clinical Microbiology and Infection*, *18*(2), E27-E30.

Turick, C. E., Knox, A. S., Becnel, J. M., Ekechukwu, A. A., & Milliken, C. E. (2010). Properties and function of pyomelanin. *Biopolymers*, *449*, 72.

Untereiner, W. A., & Naveau, F. A. (1999). Molecular systematics of the Herpotrichiellaceae with an assessment of the phylogenetic positions of Exophiala dermatitidis and Phialophora americana. *Mycologia*, *91*(1), 67-83.

Weber, S. (2005). Light-driven enzymatic catalysis of DNA repair: a review of recent biophysical studies on photolyase. *Biochimica et Biophysica Acta (BBA)-Bioenergetics*, *1707*(1), 1-23.

White, T. J., Bruns, T., Lee, S., & Taylor, J. (1990). 38 - AMPLIFICATION AND DIRECT SEQUENCING OF FUNGAL RIBOSOMAL RNA GENES FOR PHYLOGENETICS. In M. A. Innis, D. H. Gelfand, J. J. Sninsky, & T. J. White (Eds.), *PCR Protocols* (pp. 315-322). Academic Press. https://doi.org/https://doi.org/10.1016/B978-0-12-372180-8.50042-1

Winston, F. (2008). EMS and UV mutagenesis in yeast. *Current protocols in molecular biology*, *82*(1), 13.13 B. 11-13.13 B. 15.

Yoshino, K., Yamamoto, K., Masumoto, H., Degawa, Y., Yoshikawa, H., Harada, H., & Sakamoto, K. (2020). Polyol-assimilation capacities of lichen-inhabiting fungi. *The Lichenologist*, *52*(1), 49-59.

Zanne, A. E., Abarenkov, K., Afkhami, M. E., Aguilar-Trigueros, C. A., Bates, S., Bhatnagar, J. M., . . . Crowther, T. W. (2020). Fungal functional ecology: bringing a trait-based approach to plant-associated fungi. *Biological Reviews*, *95*(2), 409-433.

Zerbino, D. R., & Birney, E. (2008). Velvet: algorithms for de novo short read assembly using de Bruijn graphs. *Genome research*, *18*(5), 821-829.

1128 Zupančič, J., Novak Babič, M., Zalar, P., & Gunde-Cimerman, N. (2016). The black yeast Exophiala
1129 dermatitidis and other selected opportunistic human fungal pathogens spread from dishwashers
1130 to kitchens. *PLoS One*, *11*(2), e0148166.

1131

1132

1133

1134

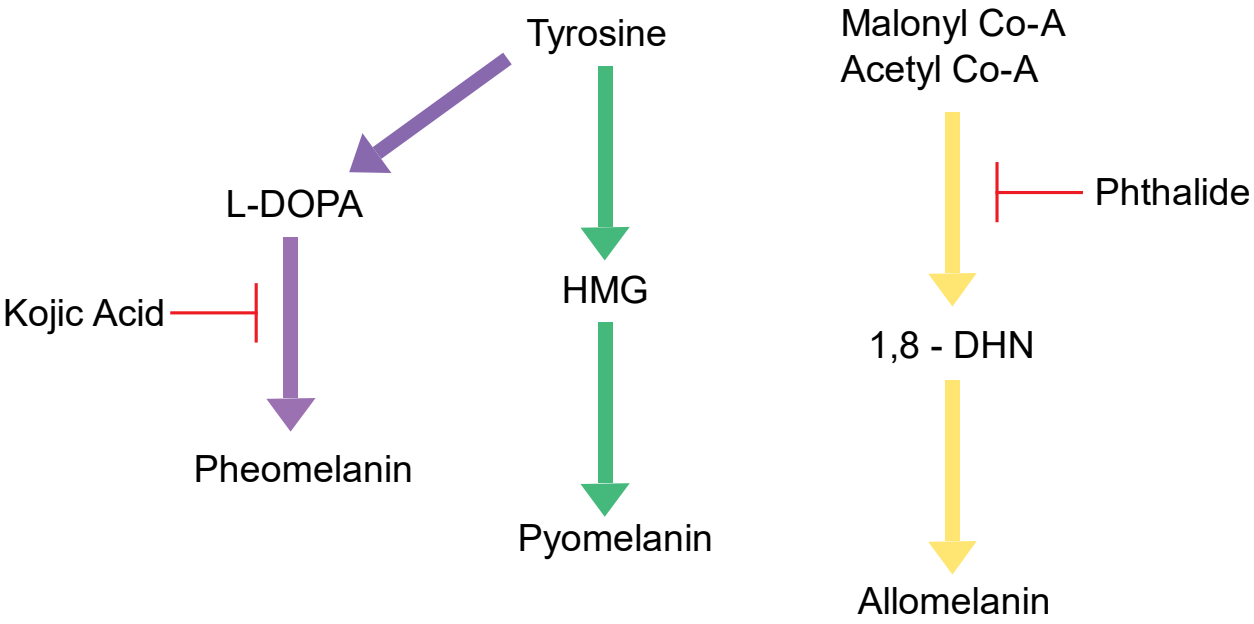

Figure 1: Visual summary of generalized fungal melanin production and the chemicals that block each pathway. Pheomelanin and Pyomelanin both use tyrosine as their starting reagent but have different biosynthesis pathways. Pheomelanin uses L-DOPA as a precursor to the final product and pyomelanin uses HMG as a precursor. Allomelanin's starting components are malonyl co-A and acetyl co-A, and its immediate precursor is 1,8-DHN. Kojic acid is a chemical blocker that blocks production of pheomelanin, and phthalide blocks production of allomelanin.

Table 1: Medias used and their compositions

Media Name	**Acronym**	**Composition (L^{-1})**
Malt Extract Agar Glucose	MAG	20 g Dextrose 20 g Malt Extract 2 g Peptone 1 mL Hutner's Trace Elements 1 mL Vitamin Mix 15 g Agar
Malt Extract Agar	MEA	20 g Dextrose 20 g Malt Extract 2 g Peptone 15 g Agar
Minimal	MN	10 g Dextrose 50 mL 20x Nitrate salts 1 mL Hutner's Trace Elements
Minimal + Vitamins	MNV	10 g Dextrose 50 mL 20x Nitrate salts 1 mL Hutner's Trace Elements 1 mL Vitamin Mix to MN
Minimal + N-acetyl Glucosamine	MN+NAG	10 g Dextrose 50 mL 20x Nitrate salts 1 mL Hutner's Trace Elements

		4.74 g N-Acetyl Glucosamine (21.43 mM)
Potato Dextrose Agar	PDA	24 g Potato dextrose powder 15 g agar (if not in potato powder)
Spider	Spider	20 g Nutrient Broth 20 g Mannitol 4 g K_2HPO_4 27 g Agar pH adjusted to 7.2 with NaOH
Yeast Extract Peptone Dextrose	YPD	20 g Dextrose 20 g Peptone 10 g Yeast Extract 20 g Agar
V8	V8	200 mL V8 Juice 2 g $CaCO_3$ 15 g Agar
Additives	**Volume/L**	**Composition**
20X Nitrate Salts/MN salts	1 L	120 g $NaNO_3$ (remove for "MN salts") 10.4 g KCl 10.4 g $MgSO_4$-$7H_2O$ 30.4 g KH_2PO_4
Hutner's Trace Elements	100 mL	2.2 g $ZnSO_4$-$7H_2O$ 1.1 g H_3BO_3 0.5 g $MnCl_2$-$4H_2O$ 0.5 g $FeSO_4$-$7H_2O$ 0.17 g $CoCL_2$-$6H_2O$ 0.16 g $CuSO_4$-$5H_2O$ 0.15 g Na_2MoO_4-$2H_2O$ 5 g EDTA (Na_4)
Vitamin Mix	100 mL	10 mg biotin 10 mg pyridoxin 10 mg thiamine 10 mg riboflavin 10 mg p-aminobenzoic acid (PABA) 10 mg nicotinic acid

Table 2: Nitrogen Sources, Concentrations, and Providers

Nitrogen Source	**Concentration**	**Catalog number**
No Nitrogen	N/A	N/A
Peptone	1% w/v	Fisher Brand: BP1420
L-Proline	100 mM	Sigma: P-0380
Ammonium tartrate	100 mM	Sigma: A2956
L-Serine	100 mM	Sigma: S4500
Sodium Nitrate	100 mM	Fisher Brand: S343
Glycine	100 mM	Fisher BioReagents: BP381

L-Glutamic acid	100 mM	Sigma: G1251
L-Aspartic acid	100 mM	Sigma: A9256
Urea	50 mM	Alfa Aesar: A12360

Table 3: Metals used and their concentration

Metal	**Concentration**	**Catalog Number**
$FeSO_4$	1 M	Fisher: I146
$CoCl_2$	0.5 M	Sigma: C-2644
$NiCl_2$	1.5 M	Sigma-aldrich: 223387
$CuCl_2$	1.5 M	Sigma: 203149
$CdCl_2$	10 mM	Fisher: 7790-84-3
$AgNO_3$	0.47 M	Alfa Aesar: 7761-88-8

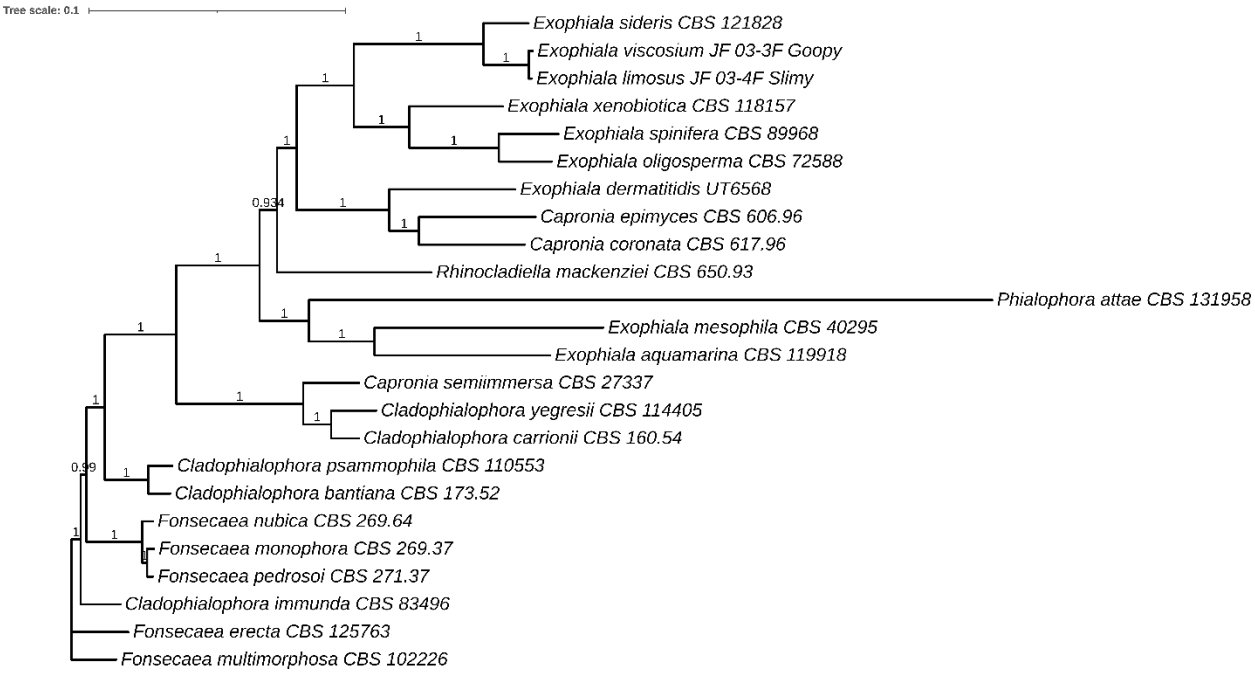

Figure 2: Protein sequence approximate maximum likelihood phylogenetic tree of taxa of the family Herpotrichiellaceae which have been whole genome sequenced and annotated. *E. viscosium* and *E. limosus* are shown to be closely related to *E. sideris*.

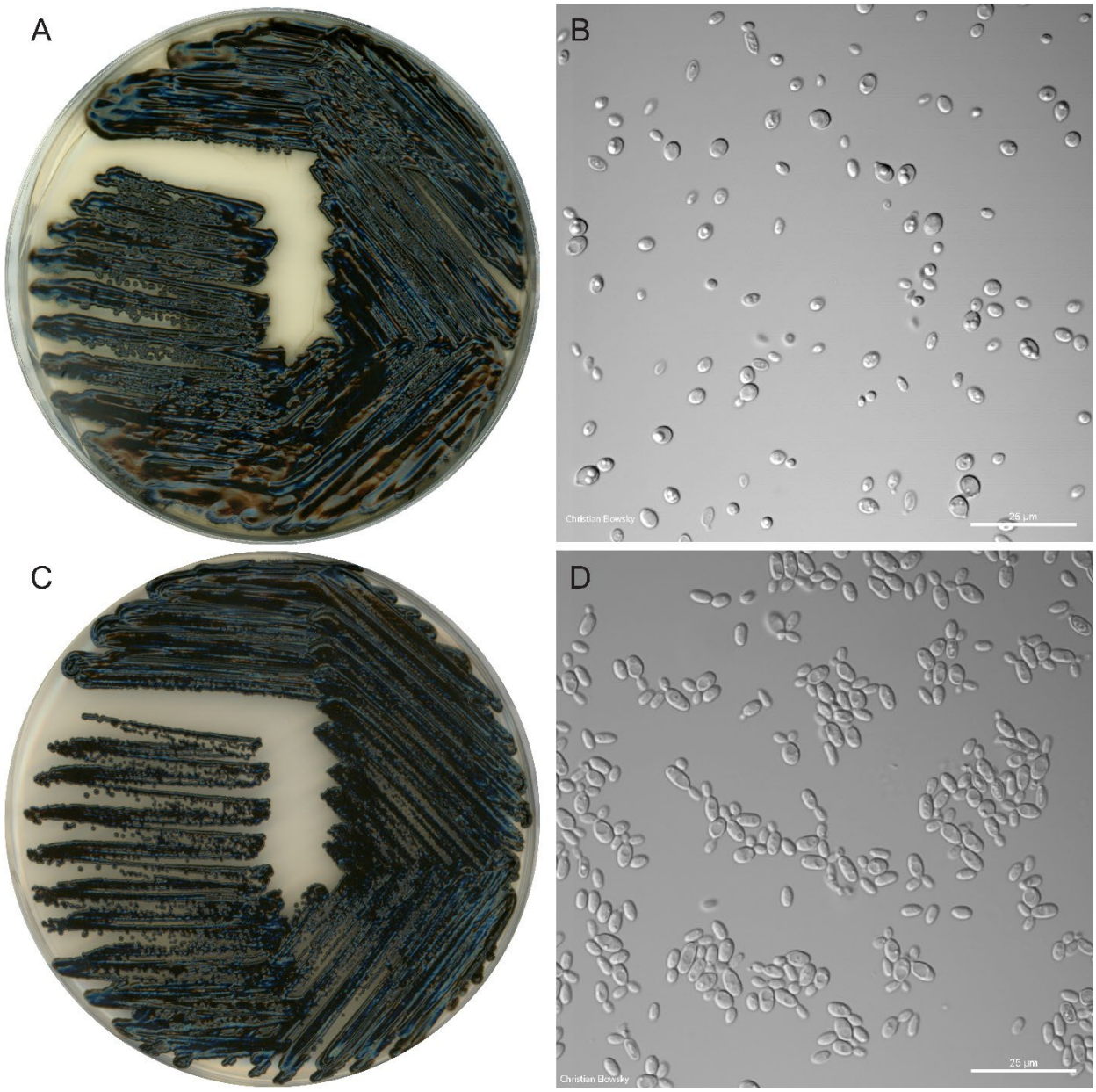

Figure 3: A) *E. viscosium* plate morphology; grown on an MEA plate for 10 days. *B) E. viscosium* cell morphology; grown in liquid MEA for 5 days; 60x objective lens. C) *E. limosus* plate morphology; grown on a MEA plate for 10 days. D) *E. limosus* cell morphology; grown in liquid MEA for 5 days; 60x objective lens. (Both plate photos and microscopy photos were taken by Christian Elowsky)

Table 4: Genome descriptions of the novel *Exophiala* species and close relatives

Genome Assembly statistics	*E. viscosium*	*E. limosus*	*E. sideris*	*E. spinifera*	*E. xenobiotica*	*E. oligosperma*	*E. dermatitidis*
Accession #s	PRJNA501636	PRJNA501637	PRJNA325799	PRJNA325800	PRJNA325801	PRJNA325798	PRJNA225511
Genome Assembly size (Mbp)	28.29	28.23	29.51	32.91	31.41	38.22	26.35

Sequencing read coverage depth	147.3x	147.8x	NA	NA	NA	NA	NA
Number of contigs	35	27	69	143	64	287	10
Number of scaffolds	30	17	5	28	15	143	10
Number of scaffolds >= 2Kbp	25	17	5	20	11	129	10
Scaffold N50	4	5	2	4	3	5	4
Scaffold L50 (Mbp)	2.24	2.89	7.9	3.79	5.04	3.39	3.62
Number of gaps	5	10	64	115	49	144	0
% of scaffold length in gaps	0.00%	0.00%	0.10%	0.10%	0.10%	0.80%	0.00%
Three largest Scaffolds (Mbp)	5.39, 4.56, 2.49	4.57, 3.58, 2.93	9.94, 7.90, 7.15	6.18, 3.93, 3.92	5.55, 5.20, 5.04	4.47, 4.29, 4.12	4.25, 4.22, 3.71
GC content (%)	51.91	49.26	49.73	49.42	51.89	50.99	51.74
Gene statistics							
Number of genes	11344	11358	11120	12049	13187	13234	9562
Gene length (bp, Average)	1840	1844	2044	1593	2072	2090	2237
Gene length (bp, Median)	1666	1671	1823	1415	1845	1879	1923
Transcript length (bp, Average)	1740	1746	1933	1483	1941	1949	2122
Transcript length (bp, Median)	1564	1574	1710	1311	1710	1735	1794
Exon length (bp, Average)	705	707	776	621	738	743	896
Exon length (bp, Median)	410	414	452	339	430	426	513
Intron length (bp, Average)	70	69	74	81	80	85	85
Intron length (bp, Median)	56	56	56	61	57	61	62
Protein length (aa, Average)	488	489	500	494	492	488	501
Protein length (aa, Median)	428	430	434	437	431	429	429
Exons per gene (Average)	2.47	2.47	2.49	2.39	2.63	2.62	2.37
Exons per gene (Median)	2	2	2	2	2	2	2

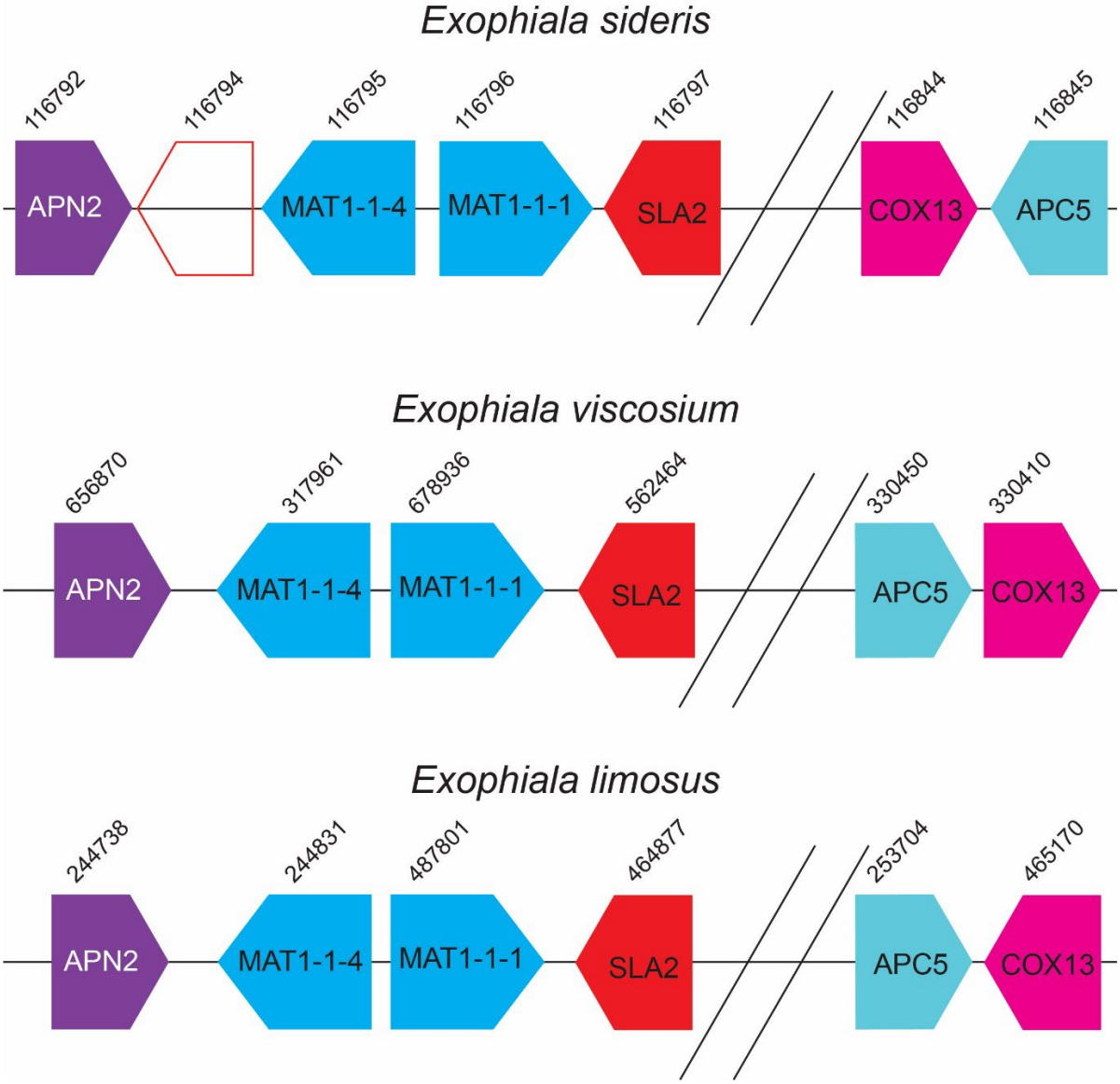

Figure 4: MAT loci gene order for *E. viscosium*, *E. limosus*, and *E. sideris*. In all three species the same genes are present within the MAT locus. *E. sideris* is indicated to have a hypothetical protein between APN2 and MAT1-1-4, whereas *E. viscosium and E. limosus* were not predicted to have that gene. Additionally, all three species have COX 13 and APC5 downstream of their mat loci, but the gene order or orientation is different amongst the three species.

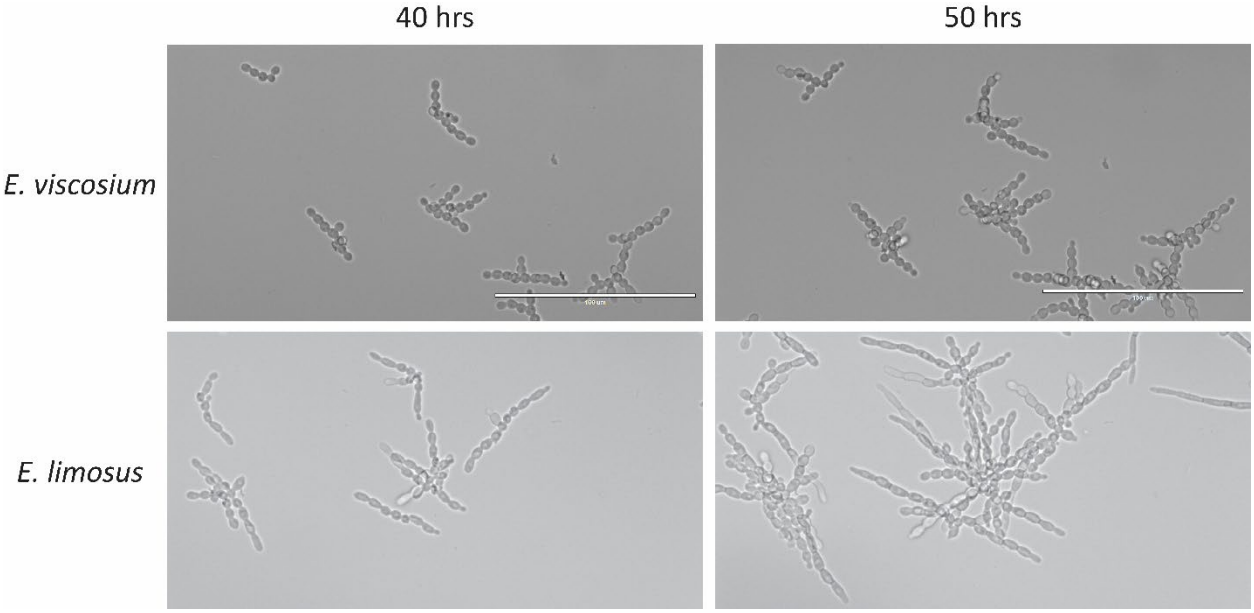

Figure 5: Budding styles of *E. viscosium* and *E. limosus*. Rate of budding is higher is E. limosus than in E. viscosium, as seen at the 50 hrs mark. Budding style is also different between the species, *E. viscosium* buds both distal polarly and proximal at close to a 90° angle, whereas *E. limosus* buds almost exclusively as a distal polar. *E. limosus*'s cells also elongate with every bud, forming almost hyphal-like structures at the 50 hr timepoint.

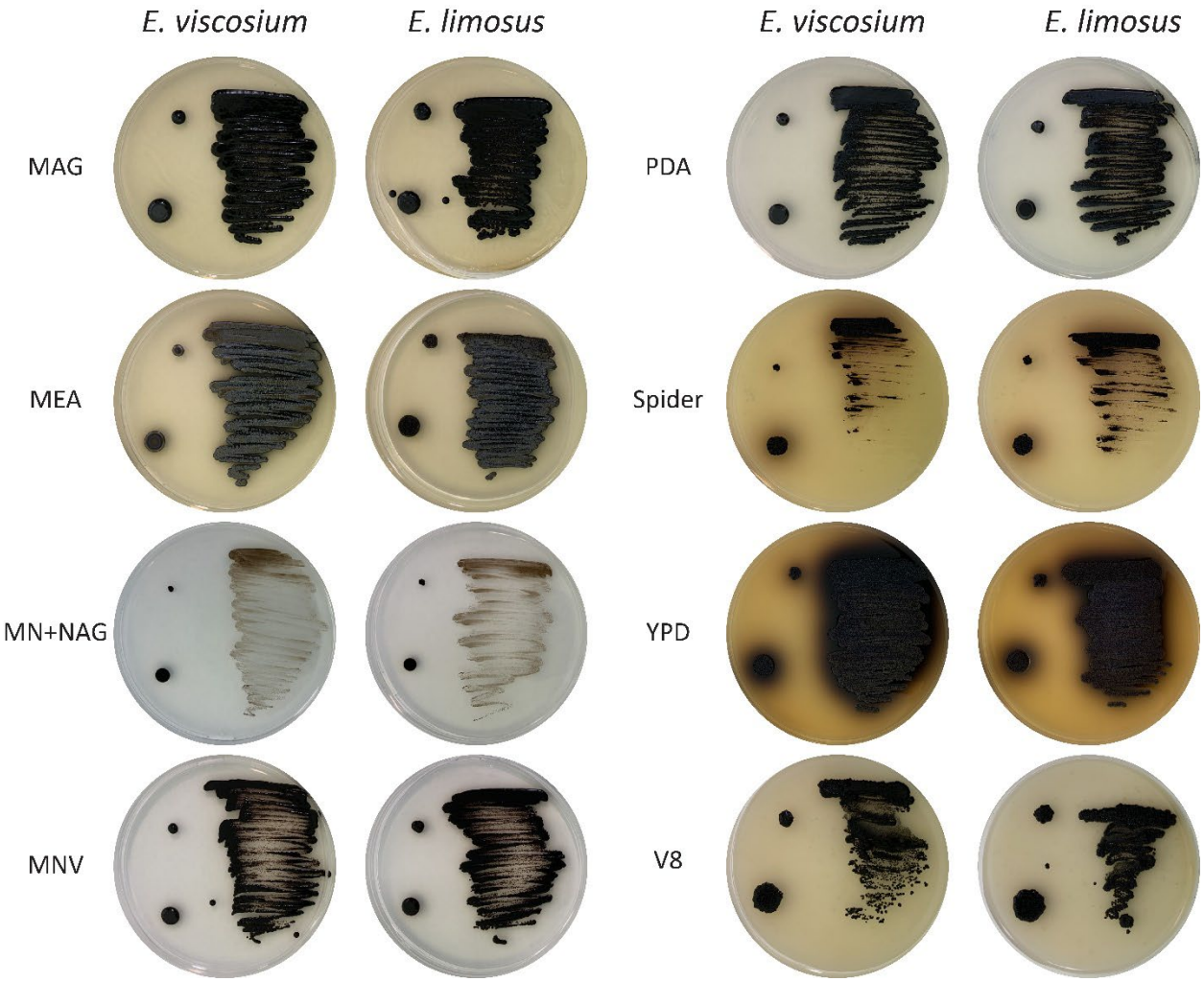

Figure 6: Growth of *E. viscosium* and *E. limosus* on eight different media types. Both species were capable of growth on all medias tested, but growth on MN+NAG showed the least amount of growth. PDA, MAG, and MNV allowed for very shiny and dark colonies to form in both species. Growth on V8 medium confirms potential for saprotrophic growth. Colorful secretions were observed on both Spider media and YPD for both species, though *E. viscosium* has more secretion into YPD than *E. limosus*.

Table 5: Carbon source utilization scores of *E. viscosium* and *E. limosus*

E. viscosium	D-galactose	D-sorbitol	Actidione (cycloheximide)	D-xylose	D-saccharose (sucrose)	D-ribose	N-acetyl-glucosamine	Glycerol	Lactic acid	L-rhamnose	L-arabinose	palatinose	D-cellobiose	Erythritol	D-rafinose	D-melibiose	D-maltose	sodium glucuronate	D-trehalose	D-melezitose	potassium 2-ketogluconate	potassium gluconate	methyl-aD-glucopyranoside	levulinic acid (leuvulinate)	D-mannitol	D-glucose	D-lactose	L-sorbose	Inositol	glucosamine	no substrate	Esculin ferric citrate
1	4	4	5	4	1	2	4	4	3	4	4	3	4	2	1	1	4	2	3	2	4	2	1	4	3	5	1	5	2	1	1	+
2	5	4	4	4	1	2	5	4	3	4	4	3	4	2	1	1	4	2	3	2	3	2	1	3	3	5	1	5	2	1	1	+
3	4	4	4	4	1	2	4	4	3	4	4	3	4	2	1	1	4	2	3	2	4	2	1	4	3	5	1	5	2	1	1	+

Avg	4.3	4.0	4.3	4.0	1.0	2.0	4.3	4.0	3.0	4.0	4.0	3.0	4.0	2.0	1.0	1.0	4.0	2.0	3.0	2.0	3.7	2.0	1.0	3.7	3.0	5.0	1.0	5.0	2.0	1.0	1.0	+
	+	+	+	+	-	V	+	+	V	+	+	V	+	V	-	-	+	V	V	V	+	V	-	+	V	+	-	+	V	-	-	+
E. limosus																																
1	4	5	4	4	2	2	4	4	3	4	4	4	4	1	1	1	4	2	4	2	3	2	1	3	3	5	1	5	2	2	1	+
2	4	5	4	4	2	2	4	4	3	4	4	4	4	2	1	1	4	2	3	2	3	2	1	4	3	5	1	5	2	2	1	+
3	4	5	4	4	2	3	4	4	3	4	4	4	4	2	1	1	4	2	4	2	4	2	1	3	4	5	1	5	2	1	1	+
Avg	4.0	5.0	4.0	4.0	2.0	2.3	4.0	4.0	3.0	4.0	4.0	4.0	4.0	1.7	1.0	1.0	4.0	2.0	3.7	2.0	3.3	2.0	1.0	3.3	3.3	5.0	1.0	5.0	2.0	1.7	1.0	+
	+	+	+	+	V	V	+	+	V	+	+	+	+	V	-	-	+	V	+	V	V	V	-	V	V	+	-	+	V	V	-	+

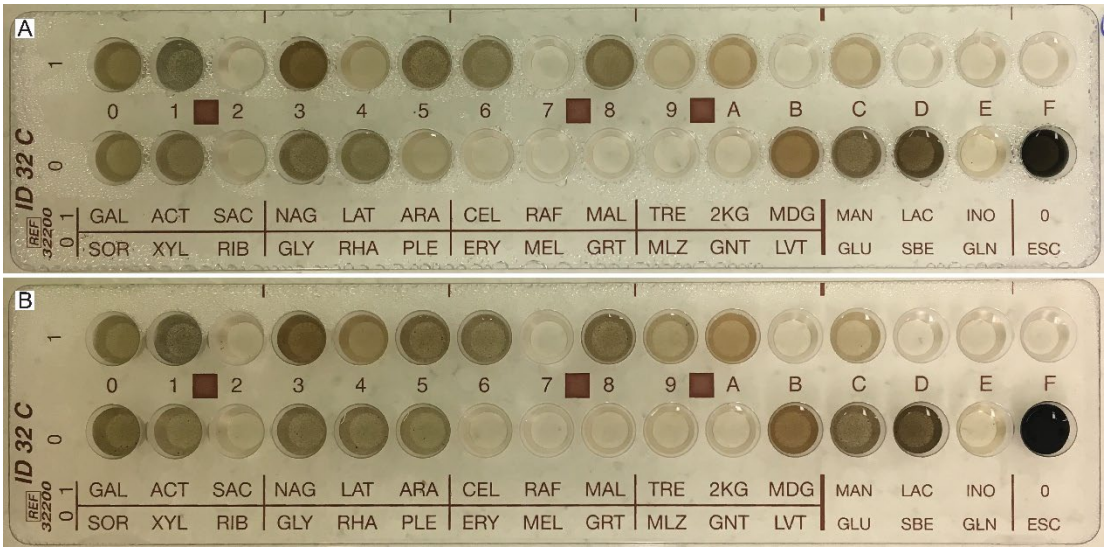

Figure 7: Growth of (A) *E. viscosium* and (B) *E. limosus* on C32 strips for determining carbon utilization. Both species were capable of using the same carbon sources, though some variations are seen. *E. limosus* was better at growing on palatinose, trehalose, potassium 2-ketogluconate, and mannitol than *E. viscosium*. *E. viscosium* was not better at growing on any carbon sources than *E. limosus*.

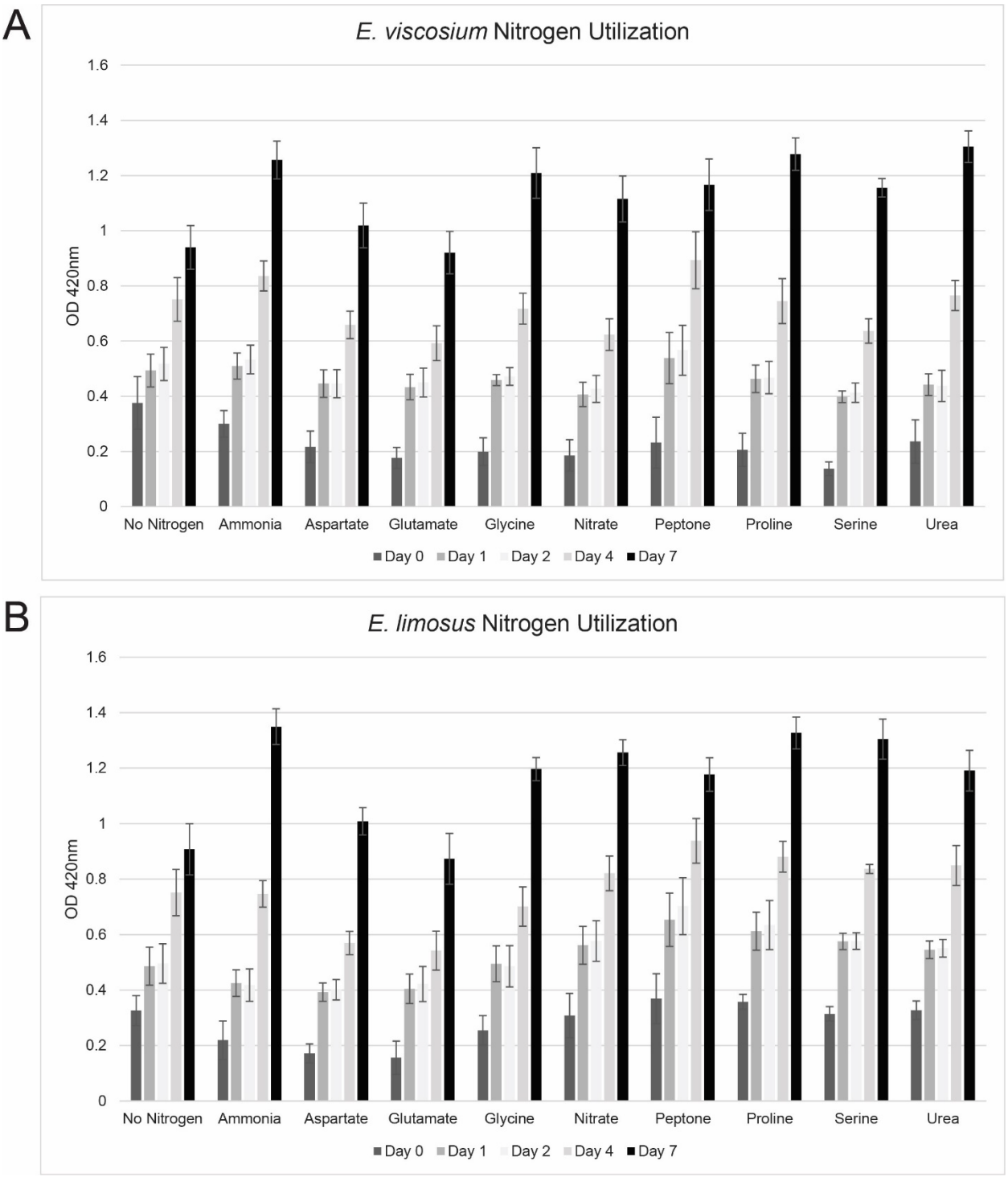

Figure 8: Nitrogen source utilization of *E. viscosium* and *E. limosus* in liquid culture. Neither species was capable of using aspartate or glutamate as a nitrogen source, as their growth amount were equivalent to no nitrogen. All other nitrogen sources tested were used by both species with varying preference. Ammonium was the preferred nitrogen source for *E. limosus*, and *E. viscosium* preferred urea and proline for nitrogen sources.

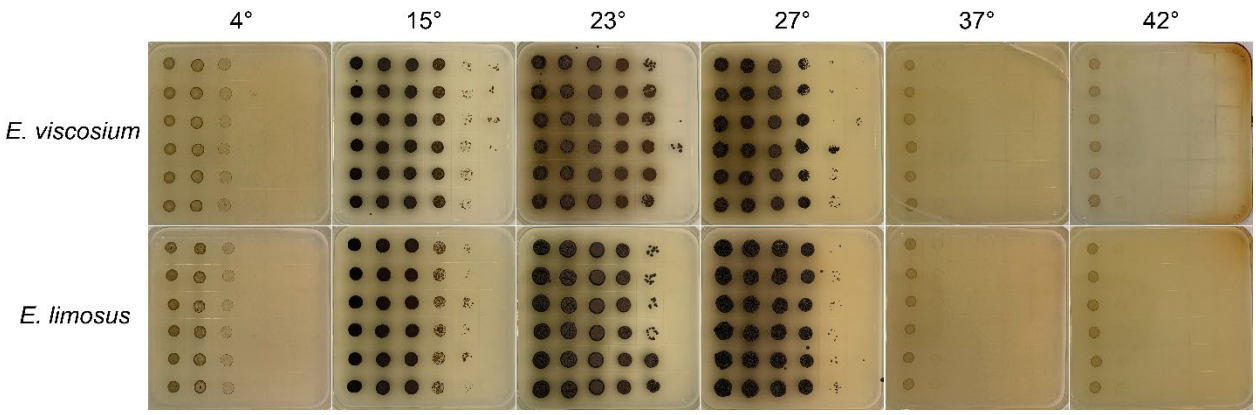

Figure 9: Growth of *E. viscosium* and *E. limosus* at varying temperatures. Neither species was capable of growth at or above 37° C, implying they are not human pathogens. Both species optimally grew at 23° C, but were capable of growth down to 4° C.

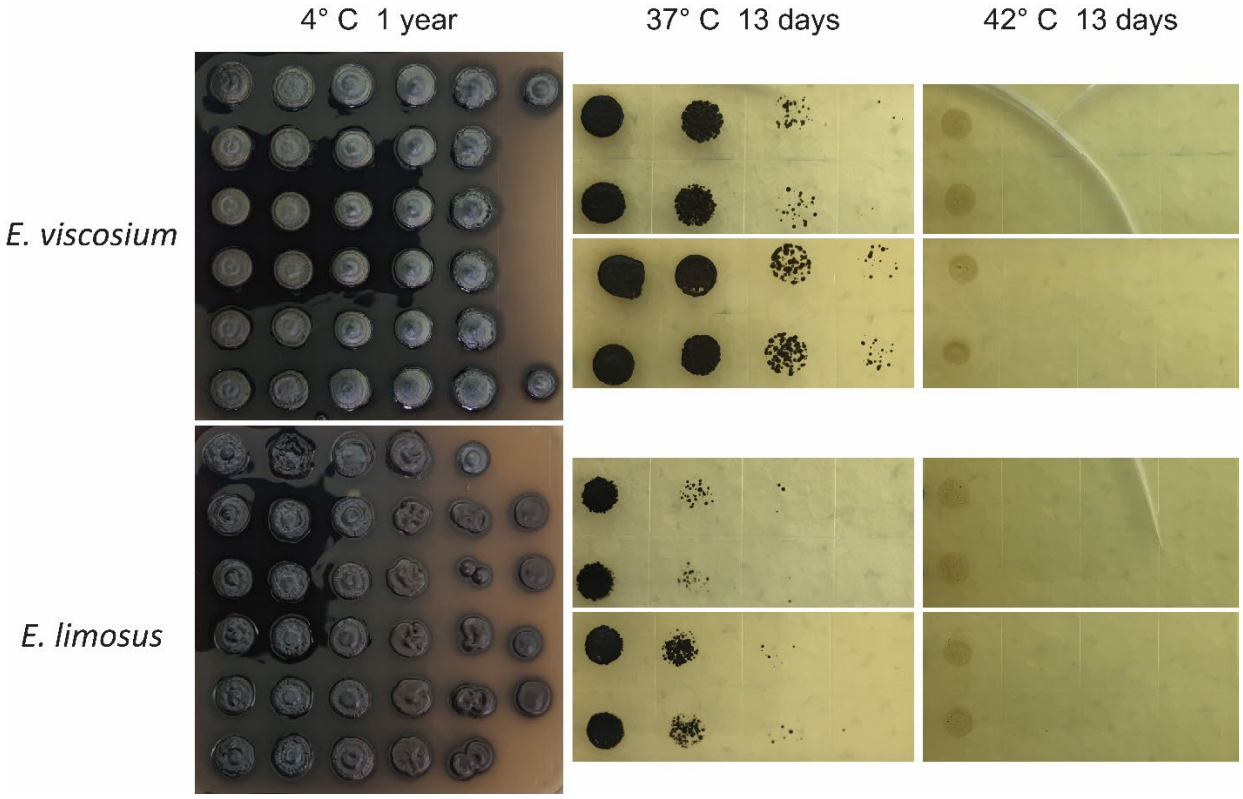

Figure 10: Growth of *E. viscosium* and *E. limosus* at the lowest and highest temperatures tested, after extended periods of time. Growth at 4° C continued for a year in both species, indicating that they can grow at these lower temperatures for extended periods of time. Additionally, we observed that while neither species was capable of active growth at 37° C it also was not too long of an exposure time to kill these cells. Whereas at 42° C neither species was capable of growth and was killed after 48 hrs of exposure.

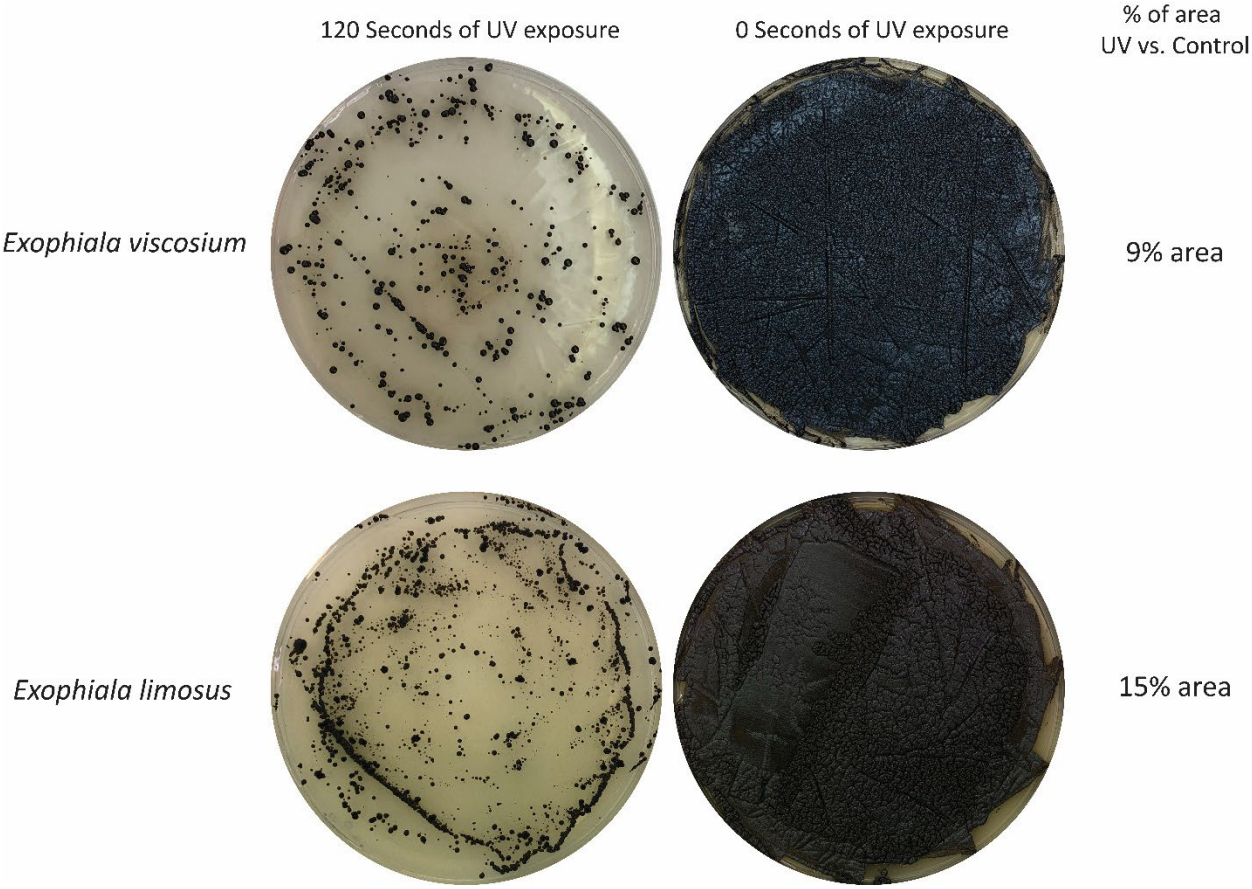

Figure 11: Difference in growth of *E. viscosium* and *E. limosus* with and without exposure to UV light. E. viscosium showed slightly less resistance to the UV exposure than E. limosus. Neither species was mutated from 120 seconds of UV exposure, normally *S. cerevisiae* and *E. dermatitidis* are incapable of growth after the same amount of UV exposure (data not shown).

Table 6: Diameter of the zone of clearing of E. viscosium, *E. limosus*, *E. dermatitidis*, and *S. cerevisiae* with various metals

Species	**$FeSO_4$ 1 M**	**$CoCl_2$ 0.5 M**	**$AgNO_3$ 0.47 M**	**$NiCl_2$ 1.5 M**	**$CuCl_2$ 1.5 M**	**$CdCl_2$ 10 mM**
E. viscosium	1.6 cm	1.5 cm	1.4 cm	3.9 cm	1.3 cm	4.5 cm
E. limosus	1.8 cm	1.8 cm	1.4 cm	4 cm	1.5 cm	3.9 cm
E. dermatitidis	1.3 cm	1 cm	1.5 cm	2 cm	2.5 cm	1.2 cm
S. cerevisiae	1 cm	1.9 cm	2 cm	2.1 cm	2 cm	2.5 cm

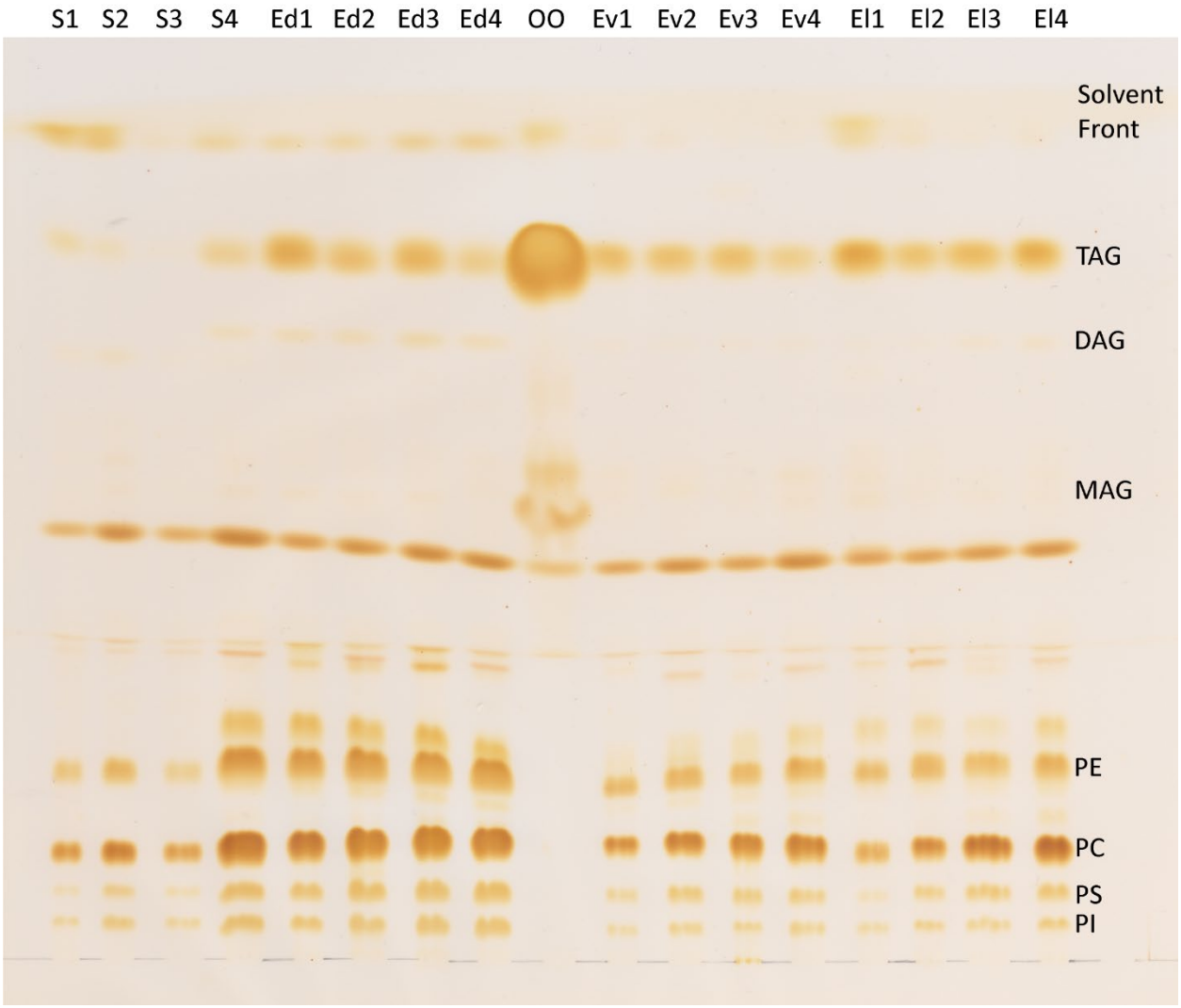

Figure 12: Lipid profile of *S. cerevisiae* (Sc), *E. dermatitidis* (Ed), *E. viscosium* (Ev), and *E. limosus* (El) using four different medias (1: MEA, 2: MEA + % peptone, 3: MEA + glycerol, 4: MEA + glycerol + % peptone). Differences in fermentable vs. non-fermentable carbon sources and amount of nitrogen source did not alter the amount or types of lipids produced by either *E. viscosium or E. limosus*. These fungi also showed no unique lipid production or any extreme accumulations of any lipids when compared to other fungi.

Table 7: Annotation of melanin biosynthetic genes for *E. viscosium* and *E. limosus*.

PKS/DHN/Allomelanin pathway		
Gene in *A. niger*	***E. viscosium* Homolog protein ID #**	***E. limosus* Homolog protein ID #**
Pks1	580617	463165
Ayg1	511449	494160
Arp2	676985	479993, 453709
Arp1	477931	210894
Abr2	603697, 153763	326274, 72468

Abr1	648725, 437535	258543, 441397
	387337, 648725	92776, 258543
	648725, 653857	258543, 102128
DOPA/Eumelanin/Pheomelanin pathway		
Gene in *A. niger*	***E. viscosium* Homolog protein ID #**	***E. limosus* Homolog protein ID #**
MelC2	140179, 643161	84855
	140179	84855
MelO	-	-
McoJ	571417	465594
McoM	571417	465594
McoD	437535	441397
McoG	437535	441397
McoF	437535	441397
McoN	653857, 649741	102128, 454148
McoI	653857, 649741	102128, 454148
L-Tyrosine degradation/Pyomelanin pathway		
Gene in *A. niger*	***E. viscosium* Homolog protein ID #**	***E. limosus* Homolog protein ID #**
Tat	606461	34310
hppD	623446	39306
hmgA	617354, 102643, 403121	430149, 483886, 431641
fahA	617341	148504
maiA	213100	198633

Figure 13

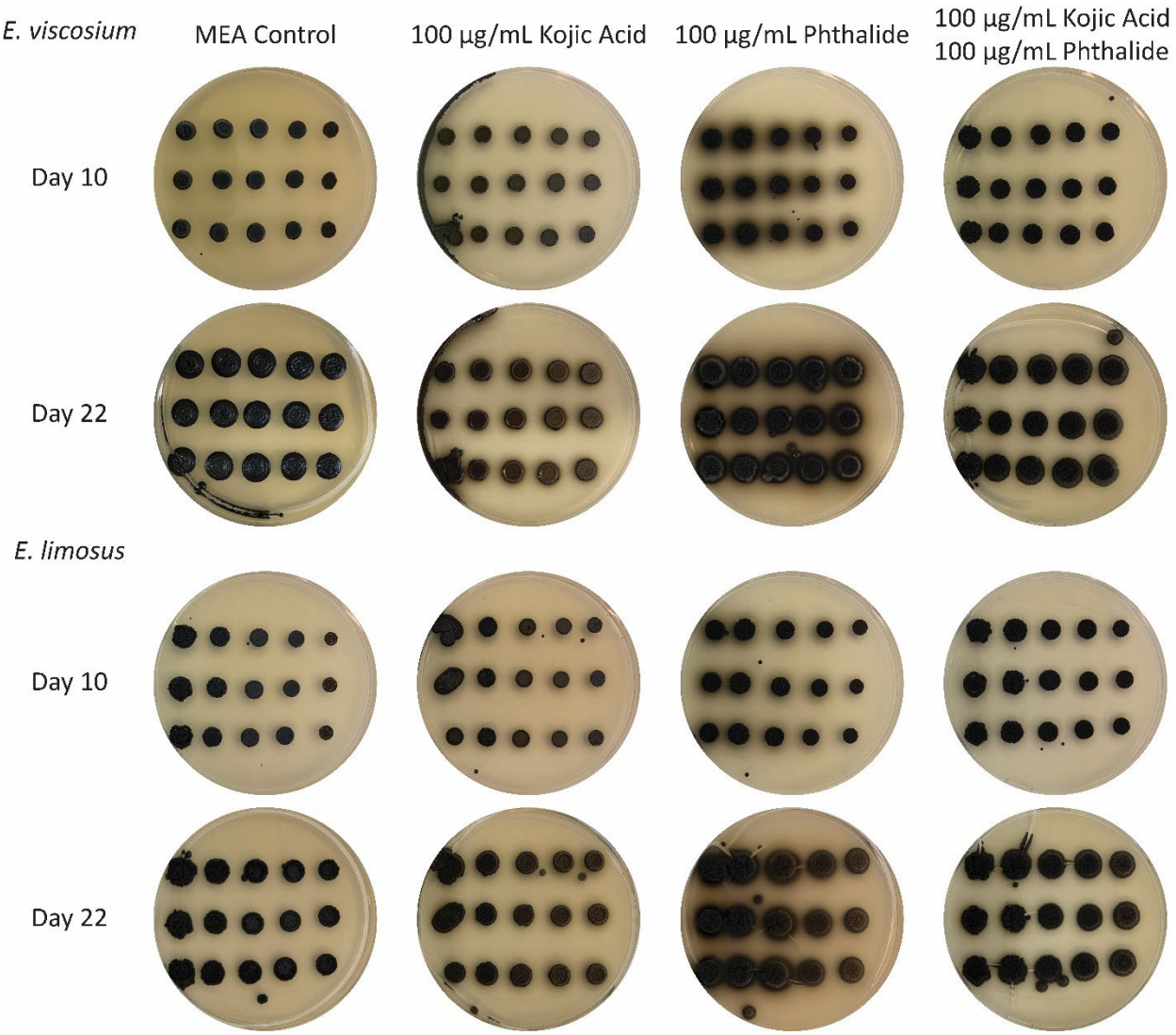

Figure 14: Growth of E. viscosium and E. limosus in the presence of melanin blockers kojic acid and phthalide. Neither chemcial melanin blocker was capable of blocking melanin production in either fungi even when both chemical blockers were used simultaneously. Additionally, use of phthalide on *E. viscosium* induced melanin secretion on a medium where this does not usually occur. The melanin halo around *E. viscosium*'s colonies on medium containing phthalide was replaced with hyphal growth after 22 days.

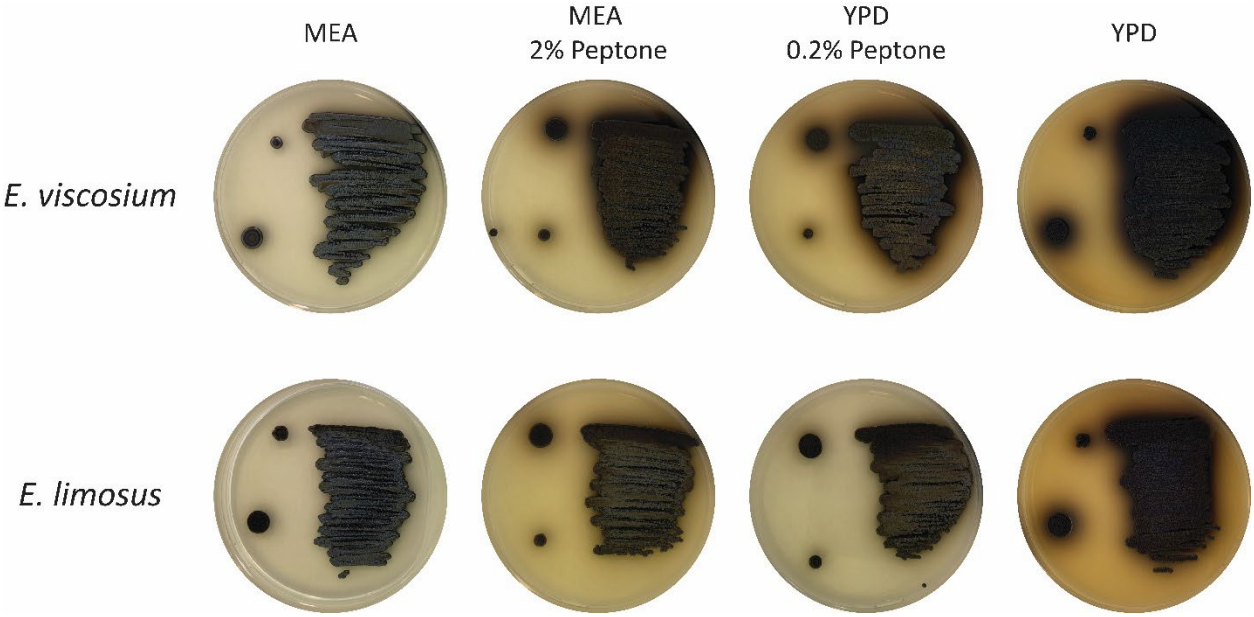

Figure 15: E. viscosium and *E. limosus* grown on MEA and YPD with different concentrations of peptone. *E. viscosium* is capable of melanin secretion on MEA with 2% peptone, which is the same amount of peptone in regular YPD. *E. limosus* was not as capable of secreting melanin in the MEA + 2% peptone, but there is a slight amount of secreted melanin. *E. viscosium* was also capable of secreting melanin on YPD with 0.2% peptone, indicating that yeast extract might have more available nitrogen than malt extract.

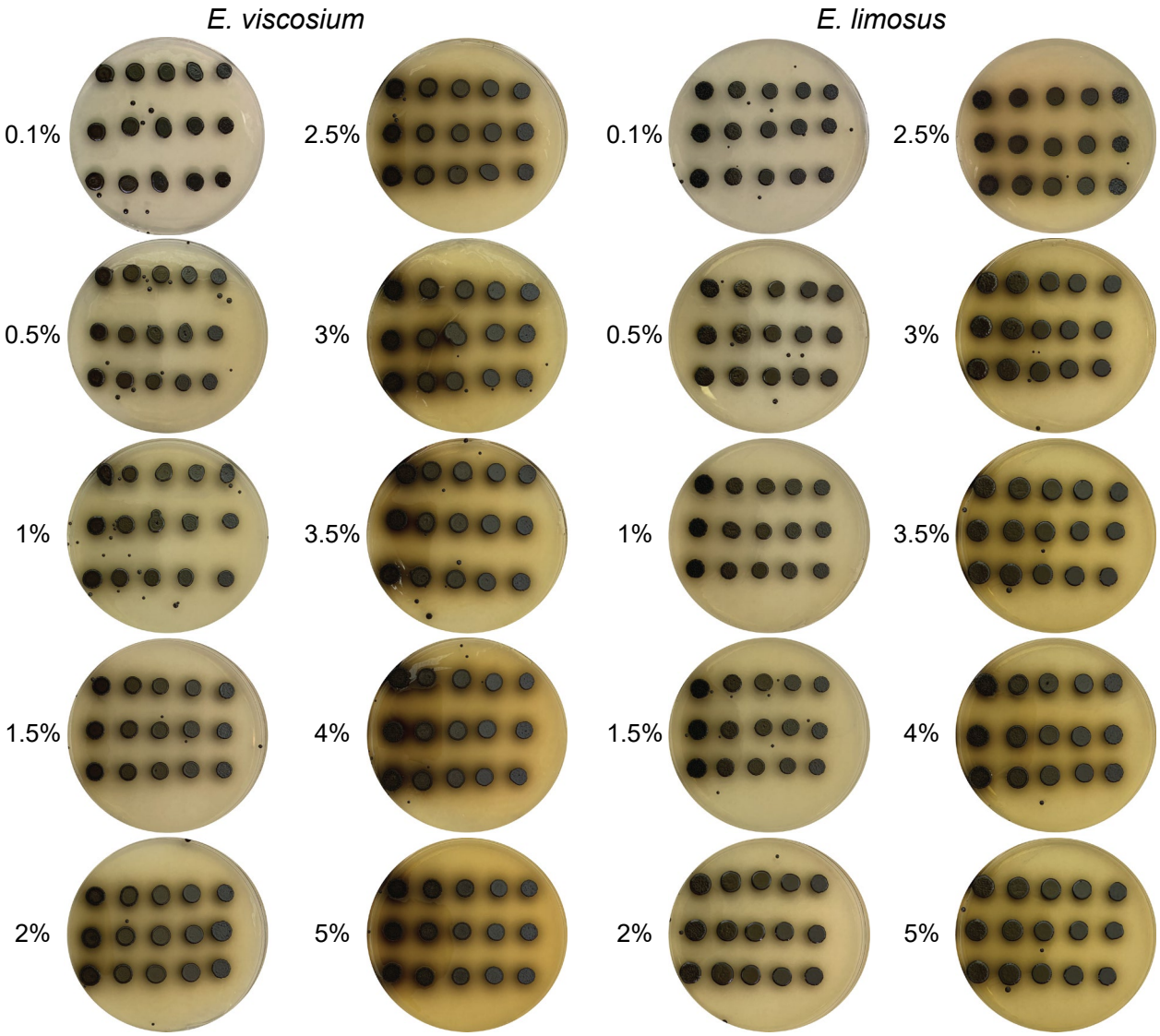

Figure 16: *E. viscosium* and *E. limosus* grown on MEA with increasing amounts of peptone. The higher the amount of peptone in the medium, the more melanin was secreted. *E. viscosium* started secreting melanin at 2%, and *E. limosus* at 4%.

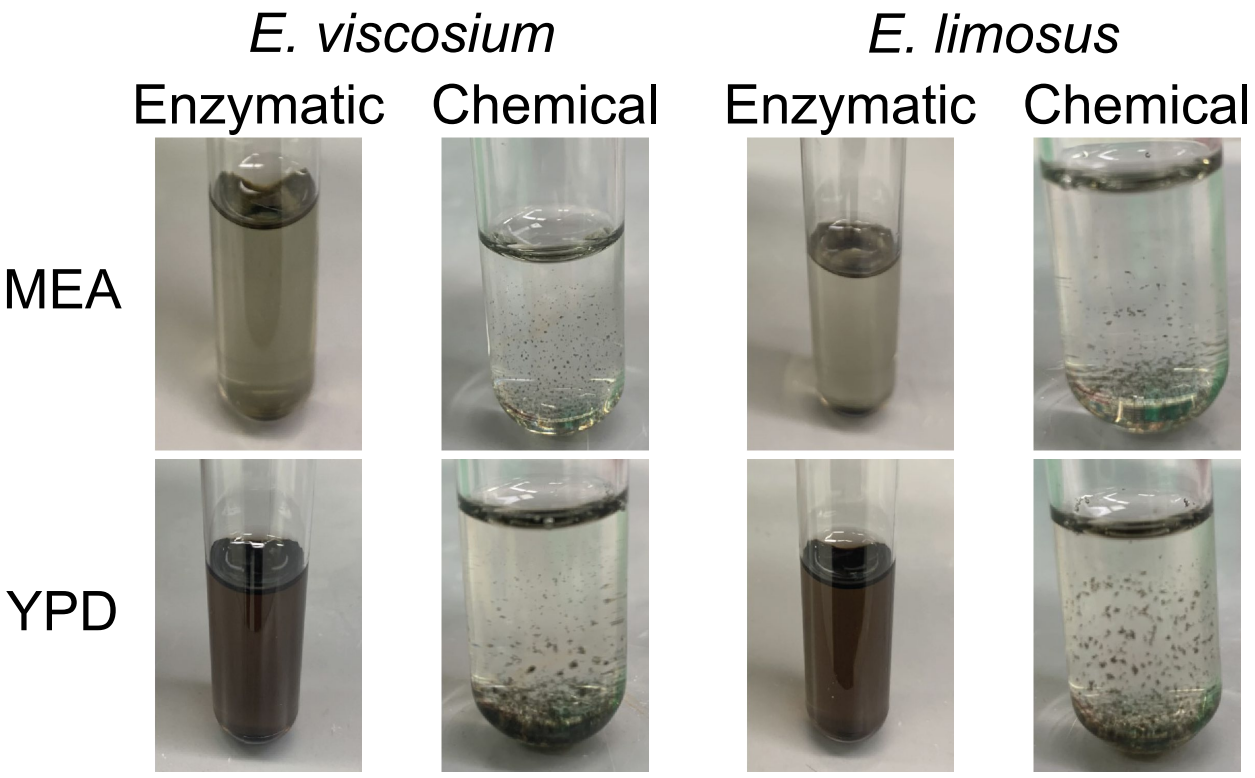

Figure 17: Extraction of melanin from supernatants of *E. viscosium* and *E. limosus* using both enzymatic and chemical methods described in (Pralea et al., 2019). Enzymatic extraction methods were incapable of extracting all the melanin, leaving behind a dark supernatant in the last step. However, melanin extracted by chemical extraction methods had complete extraction of the secreted melanin.

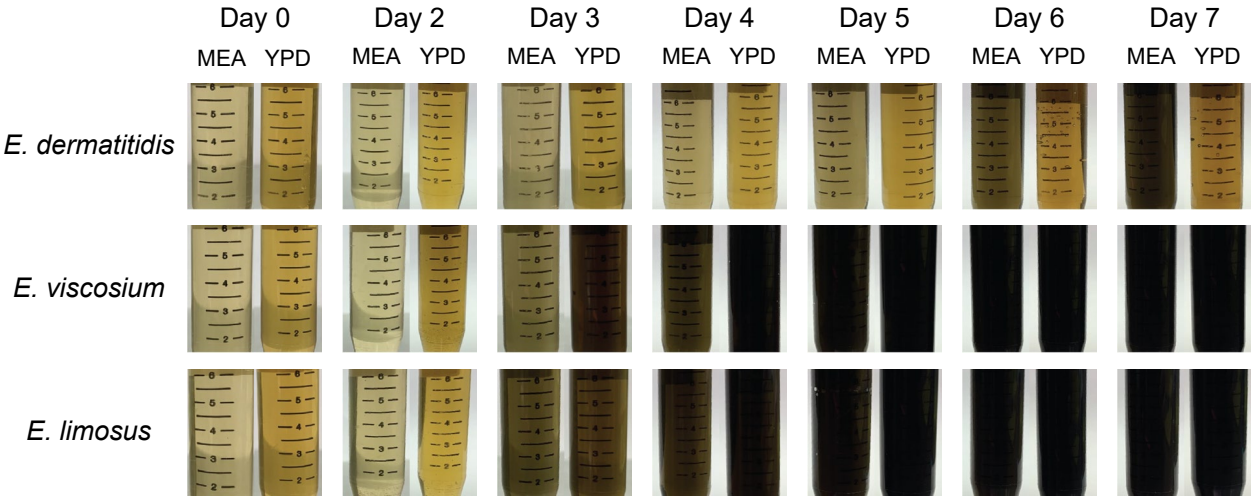

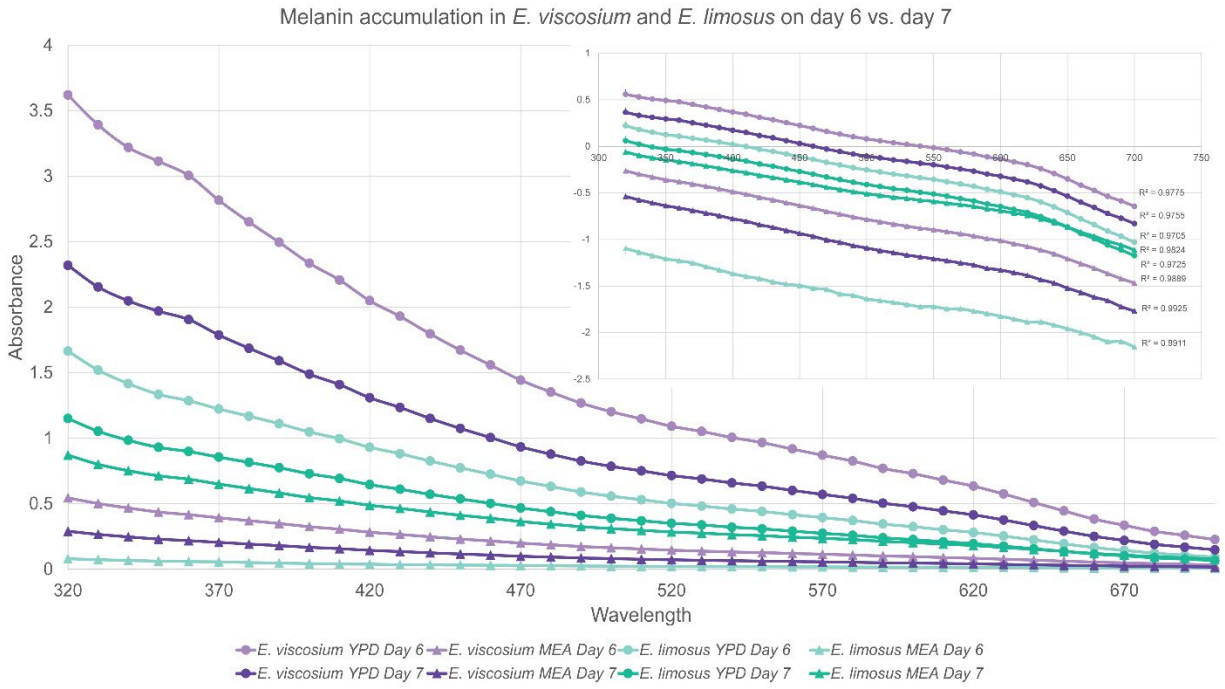

Figure 19: Day 7 results of daily melanin extraction from *E. viscosium*, *E. limosus*, and *E. dermatitidis*. All samples display typical melanin properties with full spectrum light, in that all samples have a linear regression with an R2 value of 0.97 or higher. The sample with the highest amount of secreted melanin on day 7 was *E. viscosium* in YPD. Both *E. viscosium* and *E. limosus* had more secreted melanin when grown on YPD as opposed to MEA which showed lower melanin secretion for both species. *E. dermatitidis* on the other hand had the highest amount of melanin in the supernatant in MEA than on YPD.

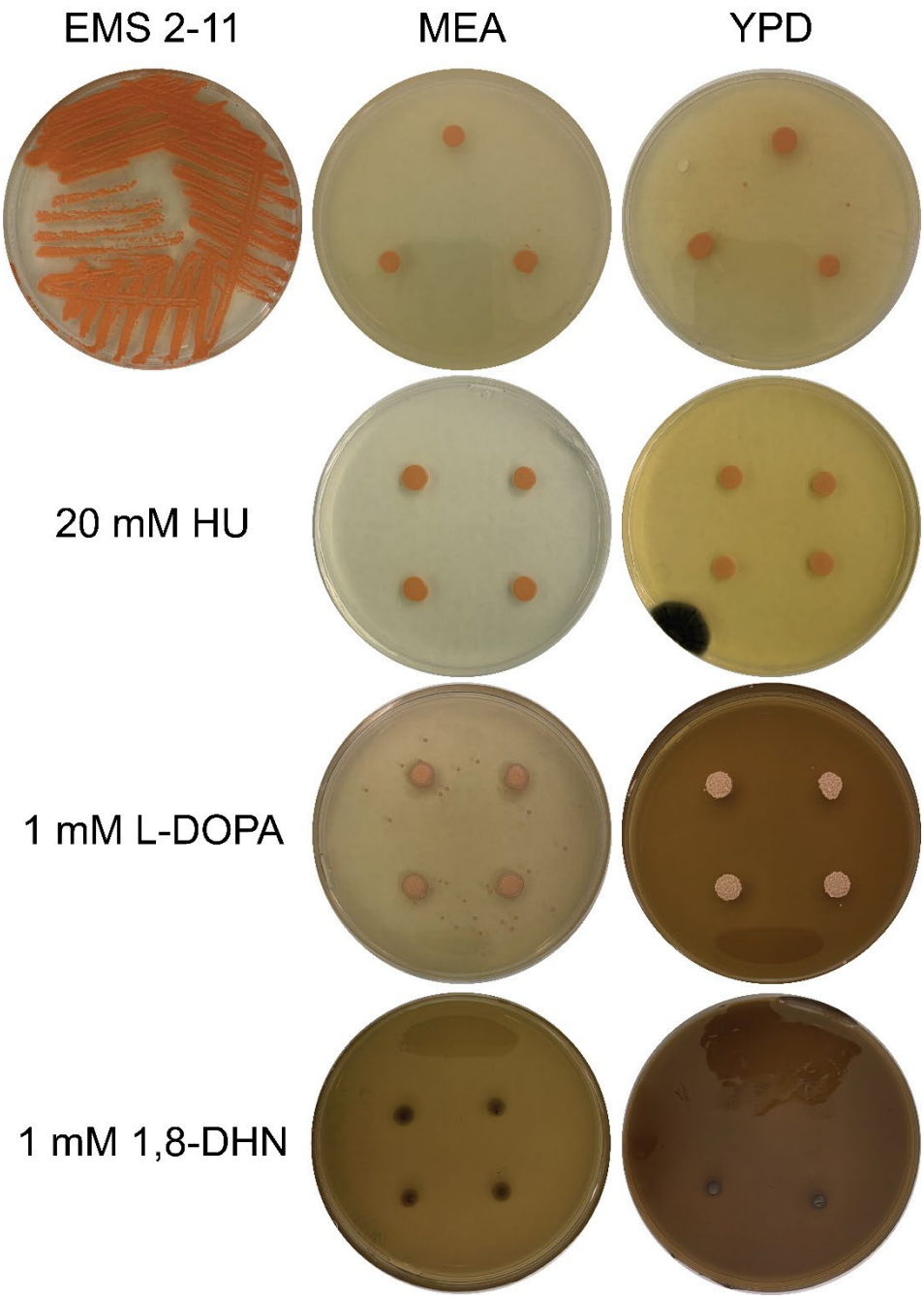

Figure 20: Phenotype of the EMS 2-11 mutant of *E. limosus* with pks1 nonsense mutation, causing melanin production to be stopped hence the pink coloration. Attempts to recover melanin production were done with Hydroxyurea (HU), L-DOPA, and 1,8-DHN. Neither HU or DOPA was able to recover the melanin in the mutant, however 1,8-DHN was able to recover melanin production in this mutant.